Research Article

Tongging Li, Zhenjia Huang, Gary Chi-Pong Tsui*, Chak-Yin Tang, and Yu Deng

Recent advances in 4D printing of hydrogels

https://doi.org/10.1515/rams-2024-0028 received November 04, 2023; accepted May 03, 2024

Abstract: 4D printing, the fabrication of dynamic 3D objects, has emerged as a frontier in additive manufacturing, benefiting from rapid advancements in 3D printing technologies and the development of new stimuli-responsive materials. Among the diverse materials explored for 4D printing, the hydrogel, renowned for its exceptional flexibility, biocompatibility, and tunable mechanical properties, is a class of soft materials well-suited for 4D printing. In addition to selecting and developing appropriate stimuli-responsive materials, it is important to devise suitable printing strategies to enable the fabrication of hydrogel-based structures that can perform complex shape-changing under external stimuli in various applications, such as soft robotics and biomedical areas. In view of this, various printing strategies, including structural design, printing scheme, and stimuli control are systematically summarized. This review aims to provide an up-to-date evolution of 4D-printed hydrogels and insights into the utilization of these printing strategies and printing techniques, such as direct ink writing, stereolithography, and two-photon polymerization, in the 4D printing of hydrogel structures for specific functions and applications.

Keywords: 4D printing, stimuli-responsive hydrogels, direct

ink writing, stereolithography, two-photon polymerization

Abbreviations

[P4,4,4,6][SPA]	tributylhexyl phosphonium 3-sulfo-
	propyl acrylate
2PP	two-photon polymerization
BIS	<i>N,N'</i> -methylenebis-acrylamide
CMC	carboxymethyl cellulose
DIW	direct ink writing
DLP	digital light processing
DMAAm	<i>N,N</i> -dimethyl acrylamide
F127-DMA	F127-N,N-dimethylacrylamide
FDM	fused deposition modeling
FFF	fused filament fabrication
LAP	lithium phenyl-2,4,6-
	trimethylbenzoylphosphinate
LCST	lower critical solution temperature
LSPR	localized surface plasmon resonance
MA-BSA	methacrylated bovine serum albumin
MAPTAC	methacrylamidopropyltrimethyl-
	ammonium chloride
MEO_2MA	2-(2-methoxyethoxy) ethyl
	methacrylate
MPL	multiphoton polymerization
MWCNT	multi-walled carbon nanotubes
NP	nanoparticle
P(DMAAm-co-SA)	poly(<i>N</i> , <i>N</i> -dimethyl acrylamide- <i>co</i> -
	sodium alginate)
P(MAA-co-	poly(methacrylic acid-co-oligo(ethy-
OFCMA)	lone alread) motherwists)

* Corresponding author: Gary Chi-Pong Tsui, Advanced

Manufacturing Technology Research Centre, Department of Industrial and Systems Engineering, The Hong Kong Polytechnic University, Hung Hom, Kowloon, Hong Kong, China; State Key Laboratory of Ultra-precision Machining Technology, Department of Industrial and Systems Engineering, The Hong Kong Polytechnic University, Hong Kong, China, e-mail: mfgary@polyu.edu.hk, tel: +852 3400 3254, fax: +852 2362 5267 Tongqing Li: Advanced Manufacturing Technology Research Centre, Department of Industrial and Systems Engineering, The Hong Kong Polytechnic University, Hung Hom, Kowloon, Hong Kong, China; State Key Laboratory of Ultra-precision Machining Technology, Department of Industrial and Systems Engineering, The Hong Kong Polytechnic University, Hong Kong, China

Zhenjia Huang, Chak-Yin Tang: Advanced Manufacturing Technology Research Centre, Department of Industrial and Systems Engineering, The Hong Kong Polytechnic University, Hung Hom, Kowloon, Hong Kong, China

Yu Deng: Guangzhou Key Laboratory of Nontraditional Machining and Equipment, Guangdong University of Technology, Guangzhou, China

lene glycol) methacrylate) OEGMA)

PAA poly(acrylic acid)

poly(acrylic acid-co-acrylamide) PAA-co-PAAm **PCEA** poly(2-carboxyethylacrylate)

PDA polydopamine

PDMA poly(N,N-dimethylacrylamide) **PDMAEMA** poly(2-dimethylaminoethyl

methacrylate)

PEGDA polyethylene glycol diacrylate PEO-PPO-PEO poly(ethylene oxide) (PEO)-poly (pro-

pylene oxide)(PPO)-PEO

PHEMA poly(2-hydroxyethyl methacrylate)

PIs photoinitiators

PNIPAm poly(N-isopropylacryamide)

PVA polyvinyl alcohol SA sodium alginate SLA stereolithography

1 Introduction

4D printing, the combination of 3D printing and the dimension of time, has emerged as a prominent research frontier in recent years because of advancements in additive manufacturing. This innovative technology empowers printed objects to undergo shape, property, or functionality changes when subjected to diverse external stimuli, such as temperature, pH, and light [1]. The applications of 4D printing span a wide array of domains, including but not limited to sensors [2,3], actuators [4,5] robots [6], circuits [7], adaptive wearable devices [8], and biomedical engineering [9-12]. Similar to 3D printing, 4D printing constructs objects the structure layer by layer, underpinned by the capability of designing complex 3D structures through computer-aided techniques [13]. A wide range of materials, including metals, ceramics, and polymers, have found application in various 3D printing techniques, such as fused deposition modeling (FDM), direct ink writing (DIW), selective laser sintering, stereolithography (SLA), and inkjet printing [14,15]. In contrast, 4D printing is still in its early stages of development and heavily relies on stimuli-responsive materials and printing techniques to produce dynamic 3D objects [16]. The careful selection of suitable stimulus-responsive materials and printing methods is essential for successfully fabricating 4D-printed objects.

Stimuli-responsive materials, such as shape memory polymers [17,18], liquid crystal elastomers [19,20], and hydrogels [21,22], are commonly used material candidates for 4D printing. Among these materials, hydrogels, physically or chemically crosslinked 3D polymer networks, can reversibly hydrate and dehydrate but not dissolve in water. This unique property enables them to absorb or expel substantial volumes of water without damaging the network structure, which

paves the way for their applications in soft actuators and soft robotics [23–26]. The aqueous environment imparts hydrogels with adjustable physiochemical properties and exceptional biocompatibility, closely resembling the characteristics of the extracellular matrix [27], applying them in many biomedical areas such as drug release [28,29] or drug delivery [30,31], biosensing [32], and cell culture [33-36]. Hydrogels have permeated various other fields ranging from environmental protection [37,38], and wearable electronics [39,40], to energy storage [41]. Additionally, stimuliresponsive hydrogels can respond to stimuli such as light [42.43], pH [44.45], temperature [46.47], electricity [48.49], and magnetism [50,51] in the manner of volume or shape change, which is similar to the process of regulating the behaviors of the 4D-printed objects. Thus, the stimuli-responsive hydrogel is a suitable material for 4D printing.

In the 4D printing of hydrogel structures, two predominant classes of printing techniques, extrusion-based printing, for example, DIW, and light-based printing, such as SLA and two-photon polymerization (2PP), have gained prominence. Table 1 compares the major features of DIW, SLA, and 2PP. Extrusion-based methods, such as FDM and DIW, rely on nozzles to extrude thermoplastic filaments or viscous precursors for constructing 3D structures [52,53]. These printing technologies are efficient for printing large 3D objects, but their printing resolutions are limited by the diameter of nozzles and filaments. In contrast, light-based printing technologies have advantages in fabricating high-resolution 3D structures and have minimal requirements on the rheology of hydrogel precursors. SLA and 2PP utilize photopolymerization to convert the monomers into crosslinked polymer networks [54-56]. This process employs spot-promoting beams from UV lasers to print 3D objects dot by dot. Exceptionally, digital light processing (DLP) is regarded as a type of SLA, but it replaces lasers with a projector to illuminate a specific area of a plane and print 3D objects layer by layer [57,58]. Although SLA has a lower printing efficiency compared to DIW, they distinguish themself by achieving superior printing resolutions. Additionally, 2PP enables the fabrication of sub-micro-meter features [59,60], and it is also advantageous for the printing of biomaterials because it utilizes near-infrared (NIR) light.

Table 1: Comparison of techniques for 4D printing of hydrogels

Printing techniques	Raw material requirement	Printing resolution	Advantage	Disadvantage
DIW	Appropriate viscoelasticity	1–100 μm	Low cost, wide range of materials	Low speed, low resolution
SLA 2PP	UV transparent NIR-light transparent	>5 µm >100 nm	Fast printing speed High resolution	Poor multi-material printing ability High cost

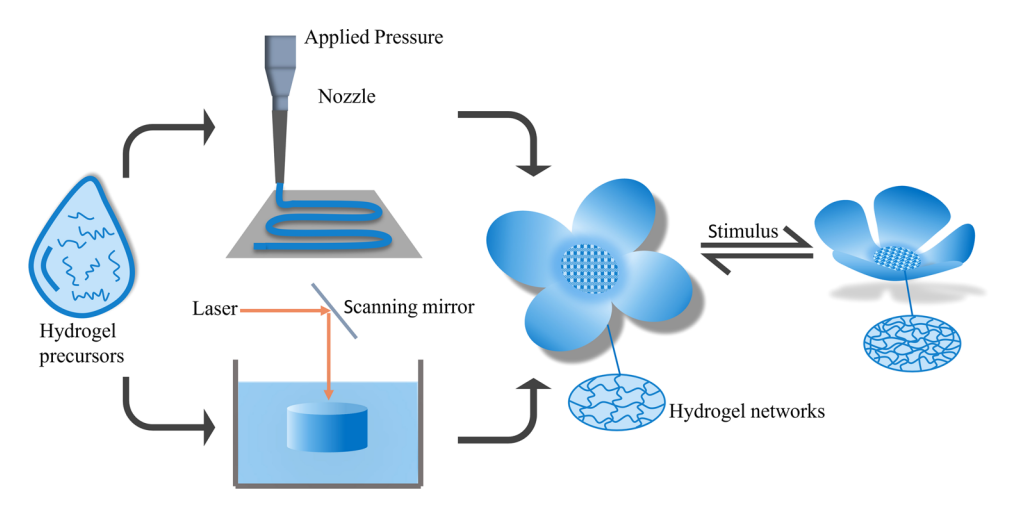


Figure 1: Schematic of fabricating 4D-printed hydrogels by DIW or SLA.

Unlike the static 3D-printed hydrogel, the 4D-printed stimuli-responsive hydrogel structures can undergo significant shape changes in response to external stimuli. To achieve complex, dynamic shape changes in 4D-printed hydrogels, additional printing strategies, such as multimaterial and multi-step printing, heterogeneous structure design, varying printing parameters, or others, are essential. Figure 1 depicts hydrogel precursors used as hydrogel inks or photoresists for DIW or light-based printing including SLA and 2PP, and printing 3D hydrogel structures capable of dynamic shape changes like blooming flowers. Although the 4D printing of hydrogel structures is also based on the 3D printing technologies of DIW or SLA and many publications elucidate the principles of these technologies, this review will not focus on these technologies in detail. The 4D printing of hydrogel structures builds upon 3D printing technologies such as DIW, SLA, or 2PP, but the distinct principles, printing schemes, size or resolution capabilities, functions, and applications of these 4D printing methods necessitate their separate investigation. This review aims to categorize 4D-printed hydrogels into DIW-printed, SLA-printed, and 2PP-printed types, and comprehensively analyze the employed materials, designed structures, 4D printing techniques, and applications across relevant studies [61-63]. The ultimate goal is to provide insights into the selection and utilization of 4D printing strategies, tailored to specific functions and applications of the 4D-printed hydrogel structures.

2 Stimulus-responsive hydrogel materials for 4D printing

Stimulus-responsive materials are the foundational components for fabricating 4D-printed hydrogels because of

their unique ability to undergo controlled swelling or deswelling in response to environmental variations. In recent research, a diverse array of stimulus-responsive materials has been harnessed to fabricate 4D-printed hydrogels using techniques such as DIW, UV-lithography, and 2PP. As depicted in Figure 2, these materials can be classified into various categories, each designed to respond uniquely to specific stimuli, including temperature, pH, humidity, ions, light, magnetic field, and others. Table 2 also provides an overview of the stimulus-responsive materials featured in recent publications, offering a comprehensive insight into their applications in 4D printing technology.

2.1 Temperature-responsive hydrogels

Among the various types of stimulus-responsive hydrogels, temperature-responsive hydrogels gained significant

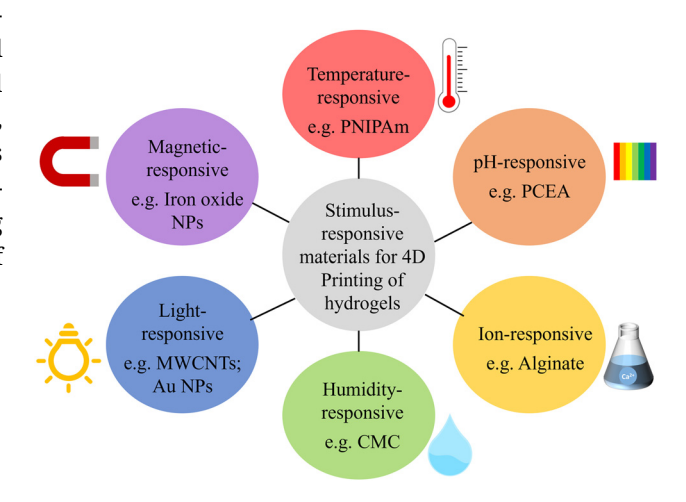


Figure 2: Overview of stimulus-responsive hydrogel materials for fabricating 4D-printed hydrogels by DIW, SLA, or 2PP.

Table 2: Stimulus-responsive materials for 4D printing of hydrogels by DIW, SLA, or 2PP

Stimuli-responsive materials	Types of responsiveness	Printing technologies
PNIPAm [64–69]	Temperature	DIW [64-69], 2PP [70]
MEO ₂ MA [74]	Temperature	SLA [74]
P(DMAAm-co-SA) [75]	Temperature	SLA [75]
[P4,4,4,6][SPA] [76]	Temperature	2PP [76]
PCEA [78]	рН	2PP [78]
SA [80], Alginate[81]	Ion	DIW [80,81]
PAA [82]	Ion	SLA [82]
CMC [87]	Humidity	DIW [87]
P(MAA-co-OEGMA) [88]	Humidity	DIW [88]
PEGDA [89]	Humidity	2PP [89]
MWCNTs [90]	Light	DIW [90]
PDA and Fe ³⁺ [91]	Light	SLA [91]
Au NPs [26]	Light	2PP [26]
Fe ₃ O ₄ NPs [99,100]	Light, magnetic	DIW [99,100], 2PP [23]
NdFeB [6]	Magnetic	DIW [6]
Iron oxide NPs [102]	Magnetic	2PP [102]
PNIPAm, PDMAEMA, MA-BSA [104]	Temperature and pH	DIW [104]
PEO-PPO-PEO and PAA [106]	Temperature and pH	SLA [106]
PNIPAm/PAA-co-PAAm [105]	Temperature and pH	2PP [105]
PDMA [107]	Temperature and pressure	DIW [107]
PNIPAm, Fe ₃ O ₄ [108]	Temperature and magnetic field	DIW [108]
PNIPAm, iron oxide [109]	Temperature and magnetic field	SLA [109]
PHEMA, Fe ₃ O ₄ [110]	pH, and magnetic field	SLA [110]
PNIPAm, nanothylakoid [111]	Temperature, light, and O ₂	DIW [111]
PNIPAm, PCEA [112]	Osmotic pressure, temperature, and pH	DIW [112]
P(NIPAm-co-AA) [113]	Temperature and pH	2PP [113]

attention in the 4D printing of hydrogels. A notable example is the poly(*N*-isopropylacryamide) (PNIPAm) hydrogel, a widely employed temperature-sensitive polymer, that is frequently printed by these printing technologies [56,64–70]. This hydrogel exhibits an apparent transition in hydrophilicity as the temperature approaches its lower critical solution temperature (LCST), typically around 32°C [71–73]. This temperature change triggers the expulsion of water and results in volume shrinkage or expansion of the PNIPAm hydrogel. The response becomes especially intricate when the hydrogel structure is non-homogeneous, leading to complex shape transformations in response to temperature fluctuations around its LCST.

In addition to the PNIPAm hydrogel, several other temperature-responsive hydrogels have also emerged in the area of 4D printing, including 2-(2-methoxyethoxy) ethyl methacrylate (MEO₂MA) [74], poly(*N*,*N*-dimethyl acrylamide-*co*-sodium alginate (P(DMAAm-*co*-SA)) [75], and tributylhexyl phosphonium 3-sulfopropyl acrylate ([P4,4,4,6] [SPA]) [76]. These materials, each with unique characteristics and LCST values, offer versatile options for achieving controllable and dynamic responses in 4D-printed hydrogel structures.

2.2 pH-responsive hydrogels

The pH-responsive polymers have emerged as another pivotal category. These materials rely on polymers endowed with functional groups capable of protonation or deprotonation, enabling them to respond to fluctuations in H⁺ or OH⁻ concentration. The acidic or basic chemical groups of the hydrogels can ionize when the pH varies above their pKa or below their pKb. This ionization leads to the increase of internal ionic repulsions and their phase would also transit from a compact to an expanded state via absorbing water [77]. Generally, the functional groups in pH-responsive hydrogels include carboxyl (-COOH) or amino (-NH₂) groups, which undergo protonation or deprotonation in an acidic or alkaline environment. One prime example of a pH-responsive polymer is poly(2-carboxyethylacrylate) (PCEA) [78]. When pH increases above the pKa of PCEA, the carboxyl groups will change from the pronated to depronated state and ionize, resulting in the swelling of PCEA hydrogels. Another example is the polyampholyte hydrogel which can show shape-changing behavior in both acid and basic environments [79]. These pH-responsive properties of hydrogels can be harnessed for

controlled and dynamic responses in 4D-printed structures by adjusting the pH of the medium. The unique properties of pH-responsive hydrogels offer great potential for diverse applications in drug delivery systems, where precise control over pH-triggered responses is critical.

2.3 Ion-responsive hydrogels

Ion-responsive hydrogels leverage ionizable groups within their composition to achieve dynamic responses. The electrically charged hydrogels exhibit volume changes in response to variations in salt concentration. Electrostatic repulsion between polymer chains is weakened because of the absorption of ions from the high-concentration salt solution, resulting in the shrinkage of hydrogels. One of the ion-responsive hydrogels is the hydrogel featured with carboxyl groups such as sodium alginate (SA) [80], alginate [81], and poly(acrylic acid) (PAA) [82]. Their carboxyl groups can chelate with ions like Ca2+ and the ion concentration can further adjust the crosslinking and properties of the hydrogels. Another ion-responsive hydrogel is the one with amino groups such as chitosan hydrogels [83]. For example, Fe³⁺ complexed chitosan hydrogels display distinct deswelling and swelling behaviors in NaCl solutions with varying concentrations [84]. This property of ion-responsive hydrogels renders them well-suited for 4D printing and different applications.

2.4 Humidity-responsive hydrogels

Humidity-responsive hydrogels constitute a unique category among stimulus-responsive hydrogels for 4D printing. In contrast to other stimulus-responsive hydrogels, the humidity-hydrogels demonstrate a distinctive sensitivity to environmental humidity levels. Their behavior hinges on the absorption or desorption of water, facilitating the transition between the dry and saturated state. When the humidity of the environment increases, the hydrogel structure absorbs water from the environment and swells via their chemical groups capable of binding water molecules. On the contrary, with the decreasing humidity, the water would evaporate from the hydrogels to the dry environment. The crosslinking densities and types of chemical groups in the hydrogel structures can affect their ability to absorb water. The higher crosslinked hydrogel structure shows less expansion [85]. Also, for example, Zeng [86] reported that the -COOH is superior in binding water molecules to -NH₂ in a neutral environment. Various hydrogels, including carboxymethyl cellulose (CMC) [87], poly(methacrylic acid-co-oligo(ethylene glycol) (P(MAA-co-OEGMA)) [88], and polyethylene glycol diacrylate (PEGDA) [89], have been fabricated into dynamic structures. This distinctive feature renders them well-suited for applications where environmental moisture is pivotal in inducing controlled responses.

2.5 Light-responsive hydrogels

The 4D-printed hydrogels can also be engineered to react to some non-contact stimuli, with light being one of the prominent examples. Unlike hydrogels that respond to stimuli such as temperature or ions, light-responsive hydrogels achieve their functionality by incorporating photothermal materials into hydrogels. Photothermal materials, such as carbon-based materials, conjugated polymers, nanostructured metals, semiconductors, and 2D nanomaterials, can be employed for the 4D printing of light-responsive hydrogels. Carbon-based materials and conjugated polymers can absorb the visible and NIR light via delocalized π electrons and release heat during their nonradiative relaxation to ground states; for instance, multi-walled carbon nanotubes (MWCNTs) [90] and polydopamine (PDA) [91]. Metal nanostructures, for example, gold nanoparticles (Au NPs) or silver NPs [92,93], can produce the localized surface plasmon resonance (LSPR) effect generated by the collective oscillations of high-density free electrons at the metal-dielectric interface, which leads to plasmonic heating when incident photons match the LSPR band [94,95]. Some semiconductor materials, such as Fe₃O₄ NPs [21], and 2D materials, like graphene [96], can utilize LSPR or nonradiative recombination of electron-hole pairs to achieve light-to-heat conversion. When the photothermal materials are exposed to light, they would convert the energy of light into heat which further causes the phase transition of the hydrogel matrix and shape change of hydrogels, for example, the bending of Au NPs/PNIPAm micro-hydrogels [26]. The 4D-printed hydrogels incorporated with these photothermal materials become light-responsive. When exposed to light, they change their hydrogel networks and shapes or functionalities due to the heat these photothermal materials convert from light. By harnessing these materials, 4D-printed hydrogels with light-responsive capabilities can unlock applications such as light-responsive biomedical devices and soft robotics.

2.6 Magnetic-responsive hydrogels

Magnetic-responsive hydrogels offer another controllable way for transformations and dynamic responses of 4D-

printed hydrogel structures. Similar to light-responsive hydrogels, the magnetic responsiveness of magnetic-responsive hydrogels derives from the magnetic materials rather than the hydrogel matrix. One common method for fabrication of the magnetic-responsive hydrogels is to blend the magnetic materials with hydrogel precursors, followed by curing to form crosslinked hydrogels [97]. The nanomaterials of transition metal alloys, and transition metal ferrites [98] can be used as magnetic materials such as NdFeB [6], Fe₃O₄ NPs [99,100], CoFe₂O₄ NPs [101], or iron oxide NPs [102,103]. In the presence of an external magnetic field, the magnetic nanomaterials generate forces to drive hydrogels to change their shapes. The shape-changing behavior can be adjusted by the distribution of magnetic nanomaterials in the hydrogels or the control of the external magnetic field [99]. This magnetic responsiveness opens up prospects for various applications, including drug delivery systems and soft robotics.

2.7 Multi-responsive hydrogels

Some hydrogels can respond to multiple stimuli by using multi-responsive materials or combining stimulus-responsive materials. One approach to preparing dual-responsive hydrogels involves the integration of two distinct stimulus-responsive polymers to prepare dual-responsive hydrogels. For instance, hydrogels responsive to both temperature and pH changes can be printed by combining materials such as PNIPAm with the methacrylated bovine serum albumin (MA-BSA) or PNIPAm and poly(2-dimethylaminoethyl methacrylate) (PDMAEMA) [104]. Similarly, combinations like PNIPAm and poly(acrylic acid-co-acrylamide) (PAA-co-PAAm) [105], poly(ethylene oxide)-poly(propylene oxide)(PPO)-poly(ethylene oxide) (PEO-PPO-PEO or F127), and PAA [106] are used to print hydrogels responsive to both temperature and pH variations.

Another dual-responsive hydrogel is derived from the thermal-responsive poly(N, N-dimethylacrylamide) (PDMA) [107], which also shows pressure sensitivity. In addition, incorporating the photothermal or magnetic NPs into the stimuli-responsive polymers is a typical method to fabricate dual-responsive hydrogels that can respond to light or the magnetic field. For instance, this method results in hydrogels that respond to both temperature and magnetic fields, as exemplified by combinations like PNIPAm and iron oxide NPs [108,109] or pH and magnetic-responsive hydrogels by poly(2-hydroxyethyl methacrylate) (PHEMA) and Fe_3O_4 [110].

Some multi-responsive hydrogels can respond to more than two stimuli. For instance, a hydrogel responsive to temperature, light, and CO₂ is printed using the thermal-responsive PNIPAm and the natural nanothylakoid extracted from spinach [111]. Another example involves a hydrogel fabricated using PNIPAm and PCEA, which exhibits responsiveness to temperature, pH, and osmotic changes [112]. Additionally, another hydrogel composed of P(NIPAm-co-AA) demonstrates sensitivity to temperature, pH, and solvent variations [113].

Table 2 provides an overview of the printing technologies employed in examples of 4D printing using stimulus-responsive hydrogels. DIW has extensive applications across stimulus-responsive hydrogel materials. Meanwhile, SLA offers choices regarding compatible stimulus-responsive hydrogel materials. Notably, many stimulus-responsive hydrogel material systems have been developed for 2PP for the generation of hydrogel-based micro- and nanostructures.

3 4D printing of hydrogels by DIW

DIW is a well-established printing technique with extensive application in the field of 4D printing of hydrogels. This printing technique operates by extruding fluid hydrogel inks through the nozzles of DIW printers to produce filaments, thus printing intricate 3D hydrogel architectures. This technique offers several advantages: DIW excels in efficiently producing macro-scale hydrogel structures with sub-millimeter resolution; unlike SLA, DIW demonstrates compatibility with non-transparent materials, including those containing high content of inorganic particles. Additionally, the multi-nozzle DIW printers can produce complex multi-material objects [114].

Similar to the process of 3D printing through DIW, the initial step in 4D printing of hydrogel structures by DIW entails the preparation of stimuli-responsive hydrogel inks. The hydrogel inks would directly affect the printing results, including printing resolution and printability. The printability, the effectiveness of the printing of designed 3D models, is intricately linked to the rheological properties of the inks, while the printing resolution is influenced by the nozzle diameter and ink filament, which, in turn, is closely tied to the rheological characteristics of the inks. Given that the nozzle size remains fixed for a particular printer, the rheology of the ink fundamentally governs both printability and resolution. Consequently, the rheological properties wield a pivotal role in determining the overall quality and feasibility of printing hydrogel objects

by DIW. Thus, strategies for the modification of ink rheology are presented in this section.

The printing of dynamic hydrogel structures through DIW involves a range of strategies. Leveraging stimulusresponsive materials is one such approach that imparts the hydrogels with the ability to expand in response to specific stimuli. Additionally, other 4D printing strategies encompass the integration of multi-materials, intricate structure design, and the fabrication of heterogeneous structures. These strategies enable hydrogels to undergo intricate shape changes, such as bending, rolling, and twisting. The distinctive responsiveness and morphing capabilities of the 4D-printed hydrogels contribute to their diverse applications.

3.1 Rheological modification of hydrogel inks

In the context of 4D printing using DIW, the rheological properties of hydrogel inks play a fundamental role, resembling the requirements of traditional extrusion molding techniques. In DIW, the printability of a hydrogel ink is intricately tied to the rheological properties of the ink, impacting both its extrudability during printing and its ability to maintain shape fidelity after printing. Before extrusion, these inks exhibit high viscosity. During the extrusion process, they undergo a significant viscoelastic transition to enable the formation of filaments under shear stress. Following this extrusion, they return to their initial viscous state to prevent any distortion or collapse of the printed 3D structures until the hydrogel structures cure [115].

Before the printing process, it is imperative to prepare hydrogel inks with the appropriate viscoelastic properties. The formulation of these inks often involves hydrogel precursors containing stimuli-responsive materials, typically derived from monomers or other small molecules. Nevertheless, they typically lack the essential viscoelasticity to serve as hydrogel inks for DIW. As a result, to prepare hydrogel inks suitable for DIW, these precursors require further rheological adjustments to achieve the necessary shear-thinning properties. Common strategies for these rheological modifications include the addition of thickeners and adjusting formulations of the inks.

Among these strategies, the use of rheological modifiers is one of the most controllable and effective methods. Specifically, adding synthesized or natural macromolecules can significantly enhance the viscous and shear-thinning properties of the inks. For instance, research has

shown that the synthesized triblock copolymer known as PEO-PPO-PEO, or Pluronic F127, can be employed as a fugitive carrier to confer shear-thinning properties to NIPAm inks [67].

It is challenging to define the printability of inks for DIW printing, as it is influenced by multiple factors [116]. However, rheology is one of the critical aspects. Some quantitative rheological parameters can aid in assessing the printability of hydrogel DIW-inks, such as the shear storage moduli (G'), shear loss moduli (G''), and phase angles σ (tan σ = G'/G''). Figure 3(a) shows the G' and G'' of NIPAm inks with varying amounts of F127 under different strains. At low strain (typically below 2%), the G' of all the NIPAm inks with F127 is significantly higher than the G''. However, as the strain exceeds approximately 2%, the G'tends to be slightly lower than the G''. The ratio of G' to G''or the tangent values of phase angles σ decrease from remarkably higher than 1 to below 1 with the strain increasing from 0.01 to 1,000, indicating that the inks change from a solid-like state to a liquid state. These thixotropic inks can be easily extruded via DIW printers to form filaments and subsequently recover to a gel-like state, benefiting the shape fidelity of the 3D structures. Adding a higher amount of F127 enhances the thixotropy of the NIPAm inks. After printing, part of the rheological modifiers can be removed via immersion in cold water because of their ability for reversible gelation [117].

Some natural materials, like alginate, are effective rheological modifiers for monomer-based hydrogel inks. As is shown in the graph of Figure 3(b), the viscosity of the acrylamide precursor solution remains constantly low under different shear rates (\dot{y}), and the shear yield stress (τ_{ν}) is low. In contrast, by adding alginate, the hydrogel ink exhibits high viscosity at low $\dot{\gamma}$, and the τ_{ν} increases significantly. This demonstrates that the ionic crosslinking of alginate can improve the printability of acrylamide-based inks [69]. The pre-crosslinking strategy can be employed in systems using monomers, such as NIPAm [64]. In another study, a natural material, thermo-responsive agar, was utilized as a thickener of inks composed of SA and acrylamide, leading the inks to be shear-thinning and printable [118].

To confer stimuli-responsive properties to hydrogels, some functional nanomaterials, for example, magnetic NPs, are introduced to the hydrogel inks. However, a common challenge in these systems is that these NPs are prone to aggregate in water, which can adversely affect the rheological properties of the inks used for DIW. The addition of certain polymeric materials can mitigate the aggregation issue and adjust the viscoelasticity. For instance, to prepare inks containing Fe₃O₄ NPs, PAA is utilized as the

8 — Tongqing Li et al. DE GRUYTER

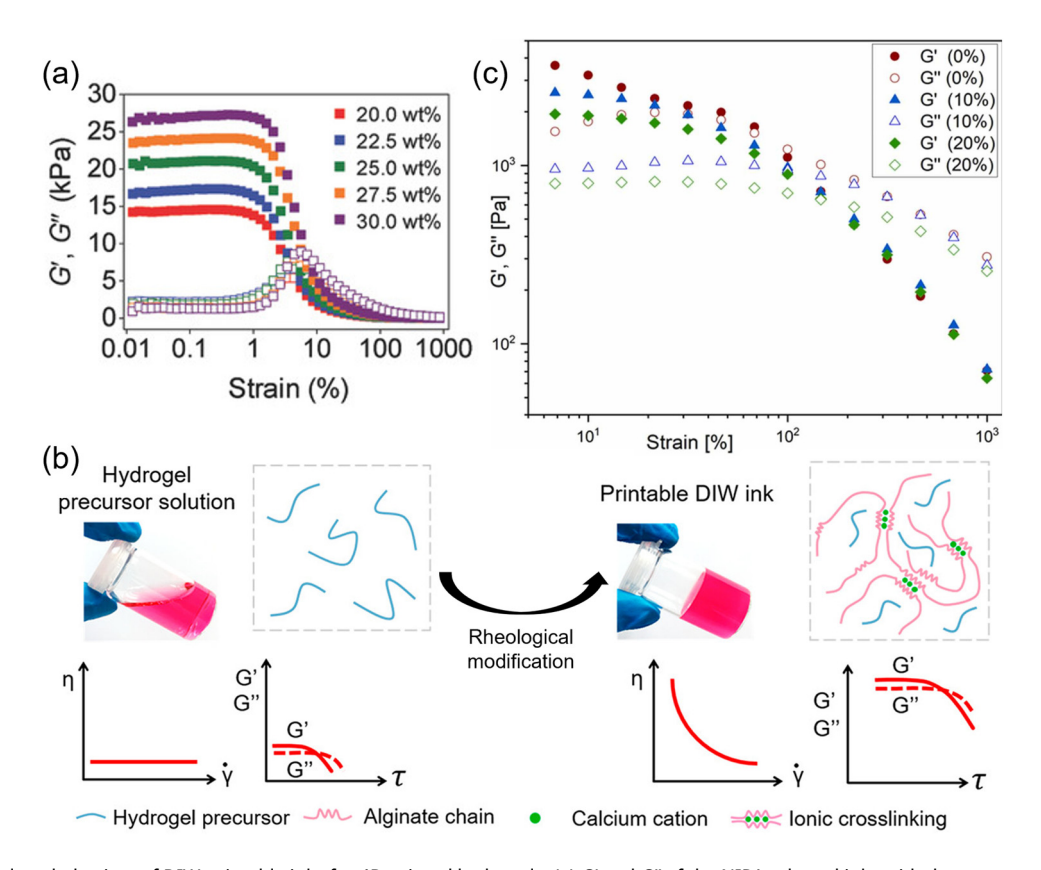


Figure 3: Rheology behaviors of DIW-printable inks for 4D-printed hydrogels. (a) *G'* and *G''* of the NIPAm-based inks with the content of Pluronic F127 varying from 20 to 30% under the shear strain from 0.01 to 1,000. Adapted with permission [67]. Copyright, 2018, Wiley-VCH under the terms of the Creative Commons CC BY license. (b) The image, molecular schematic, and rheological properties of AAM solution and those of AAM-based inks rheologically modified by alginate. Adapted with permission [69]. Copyright, 2019, American Chemical Society. (c) shear loss modulus (*G''*) and shear storage modulus (*G'*) of alginate and inks containing 0, 10, and 20 wt% of ferrofluid modified with PAA under the shear strain from 0.01 to 1,000 at the frequency of 1 Hz. Adapted with permission [99]. Copyright 2019, Elsevier.

stabilizer of these NPs, and then, the stabilized NPs are added to the alginate and methylcellulose hydrogel precursors. As shown in Figure 3(c), with the addition of these materials, the inks containing 10 and 20% of ${\rm Fe_3O_4}$ NPs still maintain suitable rheological properties conducive to DIW, as indicated by a tano value below 1. In another study conducted by Podstawczyk and colleagues [119], laponite nanoclay as a rheological modifier was incorporated in PNIPAm-based hydrogel inks. The viscoelastic properties of these inks can further be tailored by alginate and PEGDA because of interactions between laponite and them.

3.2 4D-printed hydrogels by DIW

The printability of hydrogel inks is the fundamental of fabricating static 3D hydrogels using DIW, but the realization of 4D functions of hydrogels relies on stimulus-responsive materials, structure design, multi-material or multi-step printing, or other strategies. These 4D printing strategies

and possible applications of the 4D-printed hydrogels are summarized in Table 3. These printing strategies enable the fabrication of hydrogels that exhibit dynamic behaviors such as bending, rolling, twisting, or other complex shape changes. This section thus introduces and elucidates various examples of using these strategies for 4D-printed hydrogels and the applications of these DIW-printed hydrogels.

3.2.1 4D printing strategy based on stimulus-responsive materials

In specific applications, the printing strategy based on the stimulus-responsive material strategy can satisfy the needs of simple expansion or contraction for applications such as in some drug delivery systems. Table 3 lists some examples that merely utilize the stimulus-responsive material strategy to fabricate the 4D-printed hydrogels. For instance, a dumb-bell-shaped hydrogel is printed through the combination of PNIPAm and alginate [64]. PNIPAm hydrogels undergo

Table 3: Recent research of 4D-printed hydrogels fabricated by DIW

Shape-morphing category	Shape-morphing 4D printing strategies category	Printing materials Pri	Printed structures	Types of stimuli	Potential applications	Ref.
Expansion or contraction	Stimulus-responsive material	PNIPAAm, alginate PNIPAm	Dumbell Capsule	Temperature Temperature	Soft robots, medical devices Drug delivery	[64] [65]
Complex shape changing	Multi-materials	DMA PNIPAm, PHEMA PNIPAm, PEGDA, Fe ₃ O ₄ PNIPAm, PAA, nanothylakoid	Grid Cubic box, hinges Stripes and plates Four-arm Flowers	Temperature, pressure Temperature Temperature, magnetic Temperature, light, and CO,	Sensors — Soft robots Robotics, biomedical devices	[107] [107] [68] [108]
	shear-induced anisotropy Structure design	CMC PNIPAm, alginate, laponite PNIPAm	Flower Honeycomb discs Saddle	Humidity, hydration Temperature Temperature	— Actuators Soft devices	[87] [66] [67]
	Multi-layer structure	PNIPAm, SA SA Alginate, methylcellulose PNIPAm, PDMAEMA, MA-BSA	Tendril/tentacle Tubular structures Tube-curling, helix, Cylinder	Temperature Ion Ion Temperature, pH	Soft robots Vascular stents Biomedical engineering Drug delivery	[69] [80] [81] [104]
	Stimulus control	Alginate, MC, PAA, MNPs F127-DMA, MWCNTs P(MAA-co-OEGMA) PNIPAm, Laponite, NdFeB	Tile Cone Mimosa, flower Leptasteria-like and shellfish-like	Magnetic Light Humidity Magnetic	— Actuators Soft robots and artificial muscle Medical treatment	[100] [90] [88] [6]
	Multi-step	Alginate, PAA, Fe ₃ O ₄ PHEMA	Cubes	Magnetic	Soft robotics Optical devices, sensors, cell culture platforms	[99] [120]

volume changes in response to temperature variations, while alginate contributes to ink rheology and enhances the hydrogel's mechanical properties through ion crosslinking. This PNIPAm-alginate hydrogel dumbbell exhibits substantial shrinkage when the temperature rises from 20 to 60°C yet remarkably retains its original dumbbell shape. Similarly, another temperature-responsive hydrogel incorporating Carbomer 940 as a rheological modifier is designed in a capsule shape to encapsulate a cylindrical model drug [65]. This system enables precise control of drug release rates dependent on temperature because of the temperature-responsive nature of the PNIPAm hydrogel. However, the hydrogels printed by the stimulus-responsive-material strategy are homogenous. Consequently, when subjected to varying stimuli across their entire structures, the resultant shape changes are isotropic, presenting as simple expansion or shrinkage. This characteristic, while suitable for specific applications like those mentioned, limits the broader applicability of hydrogels printed using this strategy, rendering them comparatively less common in real-world applications [80.120-123].

3.2.2 Other 4D printing strategies

In the pursuit of fabricating hydrogels endowed with complex shape-morphing capabilities, it becomes imperative to explore alternative 4D printing strategies. Many of these strategies are related to the printing process, including using multi-materials, multi-step printing, shear-induced anisotropy, and multi-layer structures, as systematically listed in Table 3. These printing strategies allow the heterogeneous 4D-printed hydrogels with diverse and complex properties. Additionally, the control over the external stimuli enables some of the 4D-printed homogenous hydrogels using stimulus-responsive-material strategy to change their shapes in a complicated manner.

The multi-material strategy facilitates the printing of heterogeneous 4D-printed hydrogels, particularly when applied in DIW. This strategy generally adopts stimulus-responsive materials and inert materials to print hydrogels in multiple steps with macro-scale interfaces between these materials. The differences in properties among these materials result in non-uniform swelling or deswelling when subjected to a varying stimulus. For instance, the bilayered hydrogel hinges are printed by thermal-responsive PNIPAm and nonactive PHEMA [68]. As the temperature increases from room temperature to 60°C, the PNIPAm component of the bilayered hydrogel hinges undergoes shrinkage, while the PHEMA component remains unaffected. This differential response causes the hydrogel hinge

to bend and fold, ultimately forming a cubic hydrogel box. A similar example involves the bilayer-structured hydrogels printed using PNIPAm hydrogel precursors and PEGDA hydrogel precursors [108].

Additionally, different stimuli-responsive materials allow the hybrid hydrogels to deform when being exposed to one stimulus since other stimuli-responsive materials remain unresponsive. As exemplified in (a) and (b), the bilayered hydrogel pad and flower exhibiting temperature-responsive and pH-responsive behaviors are designed to achieve reversible bending upon fluctuations in temperature or pH [104]. Similarly, bilayer-structured hydrogels can be printed using material combinations such as PNIPAm and nanothylakoid [111]. These hydrogels differ from the simple blending of dissimilar materials.

Given the extrusion process in DIW, certain hydrogel inks exhibit anisotropic behavior when subjected to shear forces. For instance, in a CMC-based ink, cellulose fibers have been observed alignments during extrusion, resulting in printed CMC hydrogels characterized by both crystalline and amorphous structures [87,124]. The amorphous structures, with less hydrogen bonding than the crystalline structures, show heightened swelling and deswelling tendencies, facilitating shape morphing upon hydration or dehydration. A parallel instance unfolds with NIPAm-based inks containing laponite. The induced anisotropy during printing under shear conditions enables PNIPAm hydrogels to expand asymmetrically or contract in response to temperature fluctuations around the LCST, exemplified by the self-rolling of PNIPAm hydrogel discs [66].

Innovative structural design [69] and additional printing techniques [67,81] prove instrumental in unlocking more complex shape changes in DIW-printed hydrogels. Cheng and colleagues devised artificial hydrogel tentacles embedded with channels, leading to unidirectional bending and rotation in 3D when the hydrogels are hydrated [69]. Another ingenious approach, demonstrated by Arslan and collaborators, involves varying the angle between the long axis of a bilayer structure and the direction of intrinsic curvature while growing the layers orthogonally. This strategy results in bending, coiling, and twisting of the printed hydrogel structures, with the extent of curvature transformation correlating with the angle, spanning from 0 to 45° [67]. Lai et al. [81] printed a three-layered hydrogel structure, and each layer has unique strip interspacing and angles. The layer with sparser stacking exhibits lower network density than the densely stacked ones, resulting in anisotropic expansion or contraction, while the angle between printed layers governs the deformation behavior. This angle drives the hydrogels to assume curled, twisted, or rolled configurations by varying it from 0° to 90°. Varying

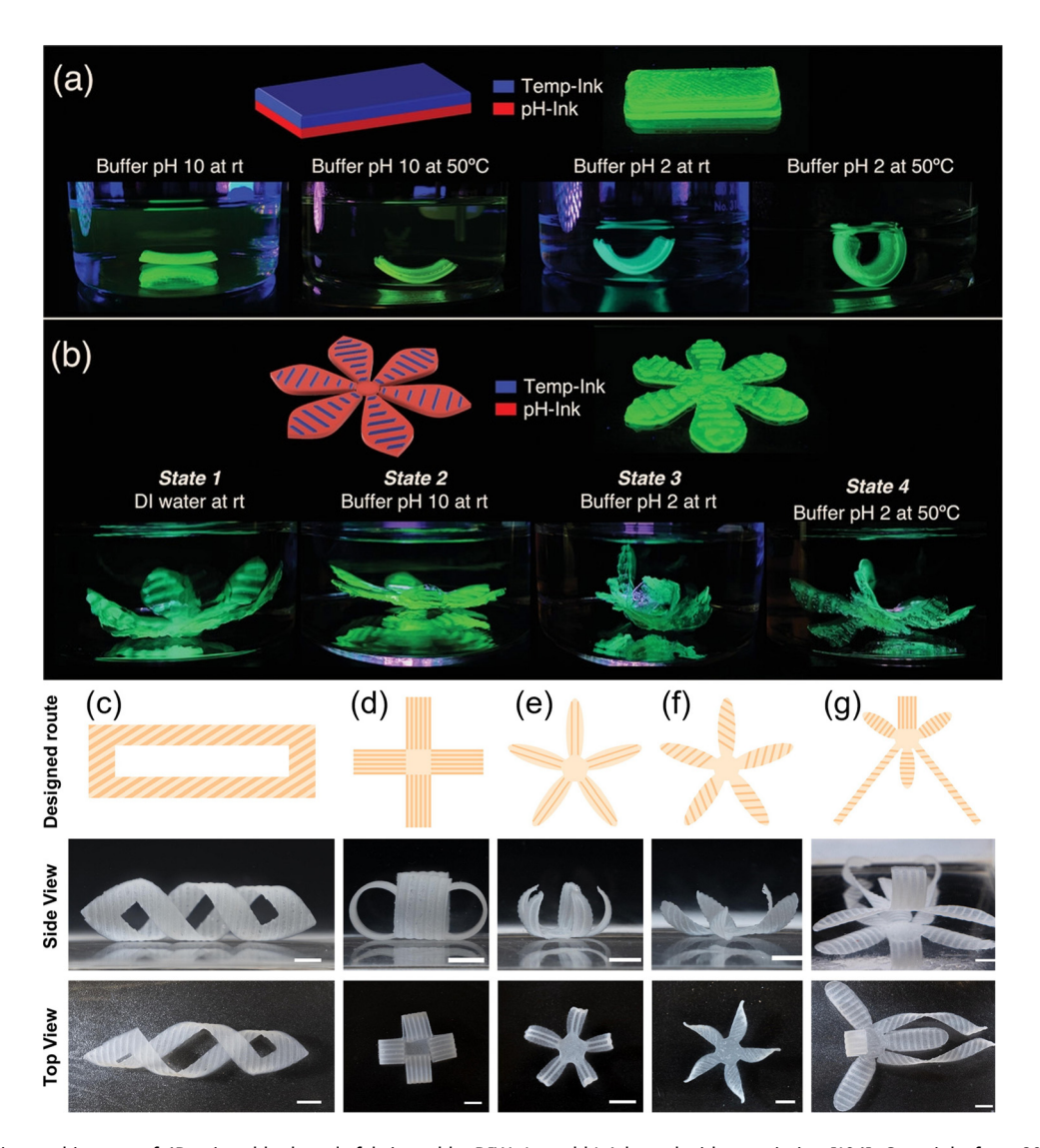


Figure 4: Design and images of 4D-printed hydrogels fabricated by DIW. (a and b) Adapted with permission [104]. Copyright from 2021, Wiley-VCH. (c-q) Adapted with permission [81]. Copyright, 2021, Elsevier, under the terms of the Creative Commons CC-BY 4.0 license.

this angle can lead the hydrogel structures to curled, twisted, or rolled configurations. They used these methods to print hydrogel structures that can transform into helices, cages, and flowers, as shown in Figure 4(c)–(g).

DE GRUYTER

Precise control over stimuli offers an effective method to govern the dynamic responses of certain 4D-printed hydrogels, particularly those designed to be magnetic responsive. Although the printing of magnetic and non-magnetic multi-layer hydrogels can induce shape morphing, with the extent primarily determined by compositional differences [99], a more straightforward approach involves the spatial control or regulation of the magnetic field intensity (H). The 4D-printed magnetic-responsive hydrogels exhibit a stronger response in regions with high H. The disparity in H can propel a global deformation of the hydrogel structure. For example, the hydrogel strips respond to the gradient magnetic field generated by a neodymium magnet, leading to controlled actuation [100]. Likewise, the magnetic-responsive hydrogel robots demonstrate horizontal rotation in the presence of a rotating magnetic field or rolling under the impact of orthogonal magnetic torque and force [6].

In another example of the printing of light-responsive 3D hydrogels, the hydrogel inks are based on a distinctive formulation designed for curing and light-responsiveness. The hydrogel networks are constructed using dimethacrylate-modified F127-N,N-dimethylacrylamide (F127-DMA), a thermal-responsive material, while the introduced multi-MWCNTs serve as the photothermal component [90]. F127-DMA offers favorable rheological properties and contains cross-linkable groups, obviating the need for additional rheological modifiers and crosslinkers. The addition of MWCNTs results in intransparence of the hydrogel ink.

Consequently, the crosslinking process employs free-radical polymerization initiated by ammonium persulfate and catalyzed by tetramethylethylenediamine, rather than UV curing. The DIW-printed hydrogel composite strip can bend because of the local exposure to NIR light [125].

between them determines the layer thickness [128]. Once a layer is fully printed, the build surface will move to print the next layer until the whole object is printed. This section aims to provide an overview of the fabrication process of 4Dprinted hydrogels by SLA and their applications, specifically focusing on using printing strategies to engineer hydrogels capable of dynamic shape morphing.

3.3 Applications

The 4D-printed hydrogels fabricated via DIW primarily exhibit macro-scale dimensions, occasionally featuring intricate microstructures. Their wide-ranging applications encompass diverse fields, prominently including soft robots, actuators, and drug delivery, as presented in Table 3. The prospects for applications are intimately intertwined with the inherent structures of these hydrogels, the types of external stimuli they respond to, and the way they go through dynamic shape-changing. Many of these hydrogels exhibit untapped potential, particularly those inspired by biomimetic designs, such as flowers [87,88,111], tendrils, tentacles [69], leptasteria-like, and shellfish-like structures [6], and other bioinspired hydrogels. For example, thermal- or pH-responsive hydrogels show promise in drug delivery, leveraging their ability to swell or deswell for drug encapsulation and release in cylinders [104] or capsules [65]. Moreover, these DIW-printed hydrogels are promising in developing wearable sensors, exemplified by the flexible device based on DIW-printed DMA hydrogels capable of monitoring human body temperature and sensing finger pressure during bending [107]. Nevertheless, the current research focus predominantly centers on harnessing the shape-morphing attributes of DIW-printed hydrogels for soft robotics applications [64,99,108].

4 4D printing of hydrogels by SLA

In the realm of 4D-printed hydrogel fabrication, SLA emerges as another prominent and widely employed 3D printing technique. SLA harnesses the photopolymerization to create polymer networks, boasting a notably elevated printing resolution compared with DIW. Over the past few decades, SLA technology has undergone remarkable development, evolving into several branches, including laser-based SLA referred to as SLA, DLP, and liquid crystal display SLA (LCD-SLA) [127], although only several examples of 4Dprinted hydrogels involve DLP and LCD-SLA. In a general SLA process, the UV light is irradiated on a building surface through a transparent window, and the distance

4.1 Composition of photoresists for 4D printing of hydrogels by SLA

The photoresists for 4D printing hydrogels by SLA generally comprise monomers, photoinitiators (PIs), crosslinkers, and solvents. Unlike DIW, the rheological modifiers are not necessary for the photoresists of SLA. The crosslinkers and solvents are the necessary components of photoresists that are similar to their counterparts for DIW. The monomers for stimulus-responsive hydrogels are the stimulus-responsive materials as listed in Table 4. The PIs are another critical component of photoresists for SLA. Due to the different SLA technologies utilizing different wavelengths of the lasers or light of SLA, the PIs vary. Usually, the PIs for UV-laser SLA and other typical SLA are triggered by UV to generate radicals. Because of the well-established advancements in UV curing, SLA can adopt various PIs such as Irgacure2959, diphenyl(2,4,6trimethylbenzoyl)phosphine oxide, and lithium phenyl-2,4,6trimethylbenzoylphosphinate (LAP) [129]. More information about PIs for SLA and 2PP can be found in the reported articles [130,131]. Additionally, since the SLA may cause overpolymerization and opacity, some light absorbers can be added to the photoresists to improve the transparency and printing accuracy in the Z-axis by controlling the curing depth [132].

4.2 4D-printed hydrogels by SLA

Following the meticulous formulation of the photoresists, the subsequent pivotal stage involves the direct 4D printing of hydrogel structures employing the SLA technique. Notably, these hydrogels can achieve volumetric transformations by utilizing stimulus-responsive materials discussed in Section 2. In recent studies, the fabrication of 4D-printed hydrogels via SLA based solely on stimulusresponsive materials remains relatively scarce. The complex changing shapes entail other 4D printing strategies, including the utilization of multi-material methods, structure design, and the printing of bi-layered or multi-layered

Table 4: Recent research of 4D-printed hydrogels fabricated by UV-based SLA

4D printing strategies	Materials	Shapes	Stimulus	Potential application	Ref.
Multi-materials	PEGDA and Fe ₃ O ₄ , PHEMA	Bilayered robot	Magnetic and pH	Drug delivery	[110]
	PEGDA and iron oxide, PNIPAm	Bilayered microrobot	Magnetic and temperature	Drug delivery Medical devices	[109]
	PEO-PPO-PEO	Bilayer slab	Temperature, pH	Medical devices	[106]
	PNIPAm, PDA PAA, Fe ³⁺	Artificial chromatophore	Light	Biophotonic device	[91]
Multi-layer structure	PNIPAm, MAPTAC	Micro-grippers	Temperature	Soft robots	[56]
	PNIPAm, PCEA	grippers	Temperature, pH, osmotic pressure	Soft robots	[112]
	P(DMAAm-co-SA)	Flower, gripper	Temperature	Soft robots	[75]
	PEGDA, PAA	Gripper, micromixer	Ion	Soft machines	[82]
Structure design	MEO ₂ MA	Strips, helices, grippers, turbines	Temperature	Robotics	[74]

structures. These 4D printing strategies to fabricate hydrogels with complex shape-changing capabilities are presented in Table 4 and comprehensively discussed in detail in this section.

Using different materials with dissimilar properties represents a straightforward approach to fabricating heterogeneous hydrogel using UV lithography, enabling these hydrogels to achieve complex shape transformations. For example, Li et al. [110] combined a magnetic-responsive Fe₃O₄/PEGDA composite layer, capable of responding to magnetic fields, with a pH-responsive PHEMA layer to engineer the functional microrobot. As is shown in Figure 4(a) and (b), this microrobot, designed to carry drug payloads, can be guided to specific positions through magnetic field manipulation, facilitated by the Fe₃O₄/PEGDA composite layer. It can release the drug when exposed to a pH environment below 3.0, triggered by the swelling of the outer PHEMA layer in response to pH changes [110]. Similarly, Go et al. [109] replaced the pH-responsive PHEMA layer with a thermal-responsive PNIPAm layer to fabricate a thermally and electromagnetically responsive microrobot which shares a similar shape-morphing mechanism with the one in Figure 4.

Another effective multi-material printing strategy for the fabrication of 4D-printed hydrogels involves combining thermal-responsive and pH-responsive materials. For instance, the integration of a triblock PEO-PPO-PEO (F127) layer with an acrylic acid layer enables the bilayered hydrogel slab to exhibit bending and even curling responses to fluctuations in temperature or pH conditions [106]. Alternatively, PAA was crosslinked with PEGDA to produce the PAA-PEGDA hydrogels, and the photothermal agent, PDA NPs, was simultaneously incorporated into the PNIPAm hydrogel. The combination of these hydrogels turns to be photoactive [91]. In

another study, a bilayered hydrogel structure, resembling flowers and grippers, fabricated through DLP technology features a polyvinyl alcohol (PVA) layer combined with a PVA-modified PNIPAm layer. This 4D-printed hydrogel exhibits enhanced toughness and heightened responsiveness to thermal changes compared to pure PNIPAm hydrogel [133].

However, 4D-printed hydrogels involving two components and two distinct materials pose challenges, including weak interfacial adhesion [74] and the time-consuming and complex fabrication process due to switching materials after printing one part. To address this, some researchers have explored the fabrication of 4D-printed hydrogel structures using a single photoresist, varying the composition within the hydrogel to print heterogeneous structures. For example, the bilayered P(DMAAm-co-SA) hydrogels were printed with two layers with different molar ratios of DMMAm to SA at 7:3 and 9:1. The layer with a higher DMMAm content shows a more considerable swelling degree, driving the bilayered P (DMAAm-co-SA) hydrogels to bend [75]. Meanwhile, The incorporation of stearyl acrylate not only enhanced mechanical performance but also allowed the tuning of the swelling properties and the LCST of the copolymerized P(DMAAm-co-SA) hydrogels because of its rigidity and the formation of the interpenetrating networks. Likewise, Valentin et al. [82] introduced ionic-crosslinked PAA into covalently-crosslinked PEGDA, producing an interpenetrating polymer network that can reversibly respond to ionic stimuli, as demonstrated in Figure 4(c) and (d). It is found there is a decrease in the swelling degree of PEGDA-PAA hydrogel with an increasing concentration of Fe3+. They combined a PEGDA layer and a PEGDA-PAA layer to print a 4D gripper that responds to FeCl₃ solution.

Another method for reducing the discrepancy between layers while maintaining the deformability of hydrogels is the fabrication of gradient-like structures. Achieving variations in crosslinking density among hydrogel layers is a practical 4D printing strategy readily attainable via SLA. Han et al. [56] utilized projection micro-SLA to print PNIPAmbased micro-gripper with bilayered claws through grayscale printing. They employed methacrylamidopropyltrimethylammonium chloride (MAPTAC) to copolymerize with NIPAm during SLA, effectively adjusting the LCST of PNIPAm hydrogels. The cationic groups in MAPTAC can enhance the hydrophilic properties of the hydrogel network, increasing the LCST of the printed PNIPAm hydrogel modified with MAPTAC to 65°C, a significantly higher value compared to that of the pure PNIPAm hydrogel. Through grayscale printing, the inner layers of each claw are exposed to higher light density, exhibiting more significant shrinkage above the LCST compared to the outer layer, allowing all claws to bend inward when the temperature increases above the LCST.

SLA enables the fabrication of 4D-printed hydrogels with varying surface area-to-volume ratios and crosslinking densities. For instance, Odent *et al.* [112] employed these printing strategies, adopting NIPAm and a pH-responsive monomer, 2-carboxyethylacrylate (CEA) to print multiresponsive hydrogel micro-grippers. Notably, Daphene Marques Solis and his colleague found that the printing temperature would affect the properties of PNIPAm hydrogels [57]. Their study demonstrated that higher printing temperature results in a decrease in the swelling capacity and an increase in LCST value.

Furthermore, strategic structural design can mitigate problems such as weak bonding force [74] and high residual stress after deformation caused by bilayer or multilayer structures. For example, Ji *et al.* [74] introduced groove structures into the hydrogel strips, incorporating helices as secondary microstructures to induce asymmetrical swelling, facilitating these hydrogels to bend and twist. Using this structure design, they achieved the onestep 4D printing of a thermal-responsive gripper using MEO₂MA *via* DLP. Figure 5(e) shows that this thermal-responsive hydrogel gripper can grasp and release a ball through water temperature adjustments near its LCST.

4.3 Applications

Because of the inherent biocompatible property, 4D-printed hydrogels fabricated by UV lithography are currently mainly applied in the biomedical area, such as drug

delivery, tissue engineering, and microrobots, as presented in Table 4. As shown in Figure 5(a) and (b), the microrobot has the potential to be used for targeted drug delivery by the control of magnetic fields [110]. However, the release process will only succeed in an environment with a pH below 3.0. Nevertheless, it provides a scheme for therapy for the targeted drug treatment of cancer. Comparably, the magnetic-responsive and thermal-responsive microrobots for drug delivery entail the temperature below LCST of PNIPAm at targeted areas [109]. 4D-printed hydrogel grippers cured by UV light are the main structure of soft robots in recent studies, and they can grab and release items via various stimulations, such as Fe³⁺ [82], temperature [56,74,75], or pH [112]. Furthermore, the DLPprinted conductive micro-hydrogels show reversible resistance change when stretched and are likely to be applied as pressure sensors [134]. Thermal and pH-responsive hydrogel scaffolds are suitable for tissue engineering [106]. The thermal-responsive hydro-turbine might be able to be used in microfluidic devices [74]. Finally, 4D-printed hydrogels cured by UV can be utilized as carriers of biomimetic materials like PDA to fabricate bio-photonic devices [91]. The combination of hydrogels and natural materials from plants or animals, like proteins, would be well suitable for cell or tissue engineering studies.

5 4D printing of hydrogels by 2PP

Photon-based polymerization leverages laser-generated photons to excite PIs, producing free radicals and initiating photopolymerization. Conventional one-photon polymerization employs UV light to excite PIs, whereas 2PP works by simultaneously absorbing two photons, halving the energy required for excitation. Also, the nonlinear twophoton absorption permits precise and localized photopolymerization of a photoresist at the laser's focal point. In comparison to UV-induced printing technologies such as SLA, 2PP is capable of fabricating intricate, sub-micrometer structures using NIR light lasers. When the photoresist is exposed to the NIR laser, the two-photon absorption of PIs triggers polymerization at the focal point of the laser beam. The movement of the laser and the build platform is coordinated to solidify each voxel in a layer before transitioning to the next, and the as-designed 3D structure is printed layer by layer until finished [135]. This section provides an overview of the printing strategies of the utilization of 2PP in fabricating micro-scaled 4D-printed hydrogels and outlines the applications of these hydrogels.

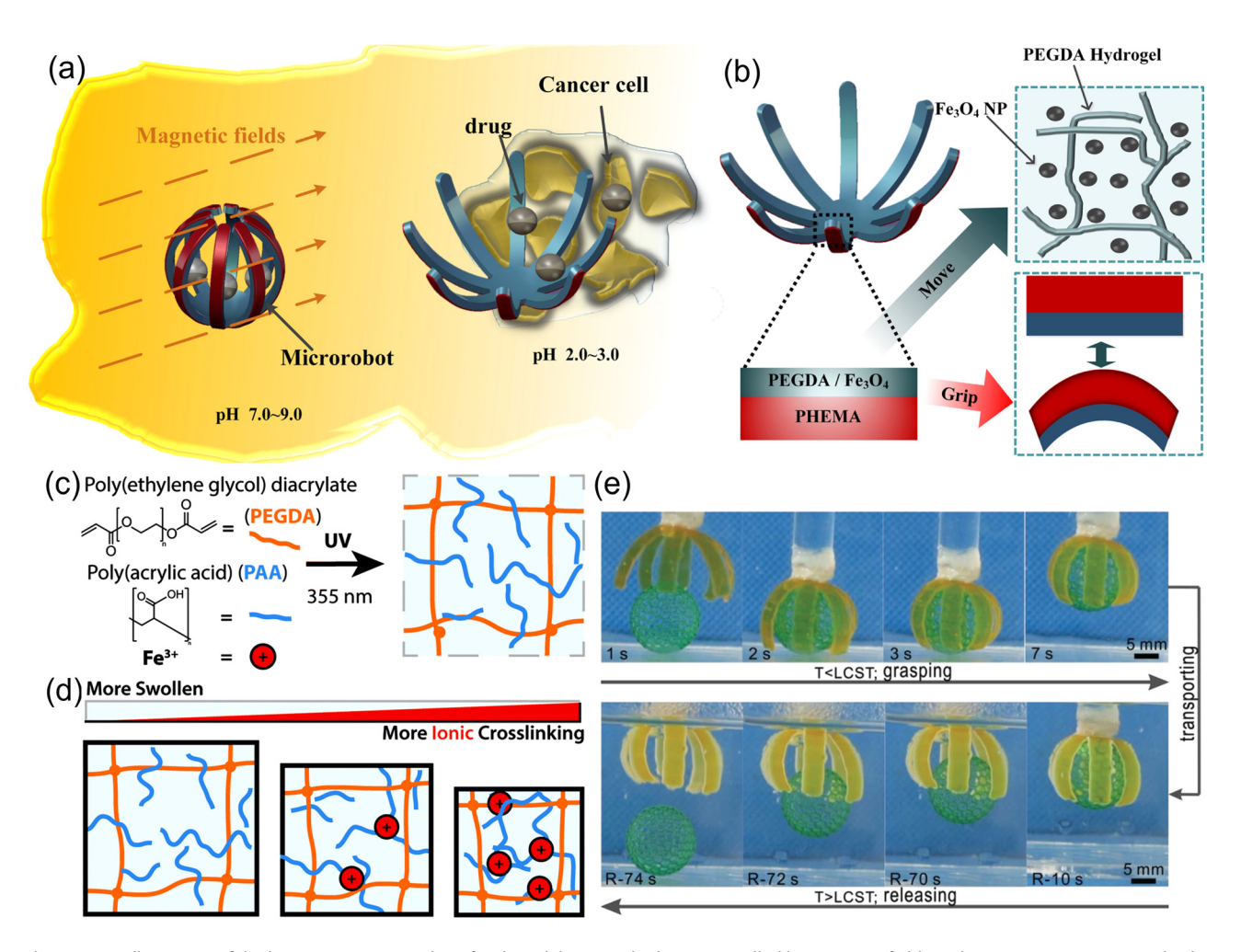


Figure 5: (a) Illustration of dual-responsive microrobots for drug delivery and release controlled by magnetic fields and pH variations, respectively. (b) The chemical composition of microrobots including the magnetic Fe₃O₄/PEGDA layer and pH-responsive PHEMA layer. Adapted with permission [110]. Copyright, 2016, IOP Publishing. (c) Schematic of the formation of UV-cured PEGDA hydrogels enhanced with PAA. (d) Schematic of the swelling degree of PEGDA and PAA hydrogel network tuned by the amount of Fe³⁺. Adapted with permission [82]. Copyright, 2019, Royal Society of Chemistry. (e) The process of grasping and releasing a ball by the hydrogel gripper. Adapted with permission [74]. Copyright from 2018, Wiley-VCH.

5.1 Photoresists for 4D printing of hydrogels by 2PP

The components of photoresists for the 4D printing hydrogels by 2PP resemble those for SLA except the PIs. As the commercialized 2PP equipment utilizes 780-nm lasers to excite the PI, it requires the PIs for 2PP to have high light absorption at 390 nm. However, current PIs are mainly designed for UV curing, and their light absorption at 390 nm is significantly lower than that at 365 nm. There are only several PIs available for hydrogel printing by 2PP, for example, LAP.

5.2 4D-printed hydrogels by 2PP

In recent studies, some examples involve the fabrication of 4D-printed hydrogels *via* 2PP based solely on stimulus-

responsive materials. Other 4D printing strategies, including the utilization of multi-material methods, structure design, and the printing of bi-layered or multi-layered structures contribute to the complex changing shapes of these 2PP-printed hydrogels. These 4D printing strategies to fabricate hydrogels with complex shape-changing capabilities are presented in Table 5 and will be comprehensively discussed in detail in this section.

5.2.1 4D printing strategy based on stimulus-responsive materials

In the earlier stage of fabricating 4D-printed hydrogels by 2PP or multiphoton polymerization, some micro-hydrogels are printed by stimulus-responsive material strategy. 2PP can print some stimulus-responsive materials mentioned

Table 5: Recent research of 4D-printed hydrogels fabricated by 2PP

Shape-morphing category	4D printing strategies	Materials	Structures	Stimulus	Potential applications	Ref.
Expansion or contraction	Stimulus-responsive material ([P4,4,4,6] Proteolytic	([P4,4,4,6] [SPA] Proteolytic-crosslinked PVA Scaffold PGGDA CFA	Micro-grids Scaffold Pvramid and dome	Temperature cell	— Morphogenesis Biocensors	[76] [136]
Complex shape changing	Multi-steps and multi- materials Heterogenous structures	PNIPAm/PAA-co-PAAm PEGDA P(NIPAm-co-AAc) PNIPAm, AU NPs	Pads fixed by micropillars Flowers, joint-like cantilever Micro-stents, micro-cages, and micro-umbrella Micropillars and micro helices Microbeams	Temperature, pH Humidity pH, Temperature, solvent Light Temperature, NIR light	Temperature, pH Hydrogel muscle Humidity Sensors, actuators, or Soft robots pH, Temperature, solvent Smart intravascular stents, Artificial cardiac valves Light Adaptive micro-devices Temperature, NJR light —	[105] [89] [113] [26]
	Stimulus control	P(NIPAm-co-Aam), Fe ₃ O ₄ NPs P(NIPAm-co-AAc), iron oxide NPs	microgripper Microrollers and microscrews	NIR light Magnetic	Microactuators microrobots	[23]

in Section 2.1 to fabricate 4D micro-hydrogels. As is presented in Table 5, there are two examples of the hydrogel materials used for 4D-printed hydrogels fabricated by 2PP in previous studies.

One of the most typical stimulus-responsive materials for 2PP printing is PNIPAm, which can be easily prepared by dissolving the NIPAm monomer, crosslinker, PI, and diluents [70]. The properties of the PNIPAm hydrogel, for example, the mechanical properties, can be tuned by varying the content of the crosslinker, which conventionally is the N,N'-methylenebis-acrylamide (BIS). Typically, the higher the proportion of BIS, the stiffer or harder the PNIPAm hydrogels are, but their responsivity and swelling capability would decrease. On the contrary, by reducing the amount of BIS, the PNIPAm hydrogel would become mechanically soft, but the photoresist would not be printable. In another study, Nishiguchi et al. [26] synthesized some multi-armed PNIPAm-based crosslinkers by RAFT polymerization. These macromolecule crosslinkers, especially the tri-allyl-functional macro-crosslinker, can increase the photoresists' viscosity to enhance the printing precision and reduce the number of crosslinking points, improving the responsiveness of the hydrogels. On top of PNIPAm, Tudor et al. [76] reported another thermo-responsive material [P4,4,4,6] [SPA] that is 2PP-printable, producing 4Dprinted hydrogels, and the polymerizable ionic monomer could form poly(ionic liquid)s (PIL) hydrogel networks. This thermal responsive material has an LCST-like behavior with a broad temperature range of phase transition, spanning from 20 to 70°C. It can dissolve other components of photoresists, including the crosslinkers and PIs, to replace the solvents which may evaporate and cause bubbles due to the heat released during the polymerization reactions. Thus, the resolution of printing can be improved to a sub-micrometer by this solvent-free photoresist. Furthermore, a cellresponsive hydrogel microstructure was constructed by MPL from norbornene-modified PVA and peptide crosslinkers [136]. Likewise, Scarpa et al. [78] utilized CEA and PEGDA to print the pH-responsive micro-hydrogel pyramids and domes. It is found that higher content of CEA or carboxyl acid groups governing the absorbing or desorbing water contributes to higher responsiveness and responsivity to the pH changes. Because of the molecular and structural design, the pyramid-like PEGDA micro-hydrogels reported by Elisa Scarpa are more mechanically robust and sensitive to pH variations than the hydrogel domes.

5.2.2 Other 4D printing strategies

2PP-printed stimulus-responsive materials can swell or deswell when exposed to stimuli. However, complex shape

changing entails 4D printing strategies, including multimaterial, multiple materials or printing steps, heterogeneous structures, and localized stimulation, as listed in Table 5.

In the earlier stage of 4D printing hydrogels by 2PP, the research mainly focuses on fabricating structured stimuliresponsive hydrogels which are generally printed by multiple materials or several steps. In 2011, Zarzar et al. [105] used acrylic acid and acrylamide to print poly(acrylic acidco-acrylamide) (poly(AAc-co-AAm)) hydrogel pads fixed by non-responsive tips on micropillars and these hydrogel pads demonstrated thermal-responsiveness and pH-responsiveness. The pH-responsive parts of the hydrogel pads show volume phase transitions occurring near the pKa of acrylic acid, around a pH of 4.25. When the temperature or pH changes, the PNIPAm or P(AAc-co-AAm) pads would expand or contract, driving the tips to bend inward or outward. Lv et al. [89] fabricated humidity-responsive PEGDA-based microstructures, mimicking stomata's closing and opening behaviors, demonstrating that the homogeneous structure of one material can only expand or contract. They also reported the microstructures of binary codes combining the active PEGDA and the inert poly(butyl methacrylate) to fabricate hydrogel micropillars in two steps. This 4D printing strategy for 2PP fabrication utilizes the difference in properties between the stimulus-responsive hydrogel and inert hydrogel to complete complex motion, but the printing process needs two steps.

Another strategy is fabricating heterogeneous structures with one material in one step. Jin et al. [113] adopted the strategy of heterogenous crosslinking density produced by the difference in exposure dose between inner and outer layers to print multiple stimuli-responsive hydrogel microstructures. Via this strategy, they utilize acrylic acid to copolymerize with NIPAm during the printing process by 2PP, and the printed AAc-co-NIPAm hydrogels could undergo a sudden and noticeable volume change at the pH of about 8.5. As a result, the printed hydrogel micromachines show different degrees of expansion or contraction when pH, type of solvents, or temperature varies, leading to complex shape morphing. Figure 5(a)-(c) presents the structures and shape changes of the micro-stent, micro-cage, and micro-umbrella, which can uniaxially contract, biaxially contract, and fold, respectively.

Programmed crosslinking density within the microstructures is another strategy for one-material and onestep 4D printing hydrogels by 2PP. For example, Hippler et al. [70] used gray-tone lithography to print the thermalresponsive PNIPAm hydrogels by a single type of photoresist in one step. They also found that hydrogels printed at the laser power of 37.5 mW have one order magnitude of

the thermal expansion coefficient higher than those printed at 30 mW, which leads to the hetero-microstructured hydrogels that can be actuated by locally focused light. Bilayered hydrogels or bi-material structures have some drawbacks, including simple shape changes and weak interaction force between the interfaces of layers. In this scenario, another 2PP printing strategy named programmed printing density was adopted to print micro-hydrogels with gradient crosslinking densities [26]. In the study conducted by Akihiro Nishiguchi and his colleagues, they first synthesized the multi-armed macro-crosslinkers which improve the printability so that the difference in crosslinking density can be enlarged attributed to the exposure dose of the laser. By varying the hatching or slicing distance at different parts of the microstructures, they printed some micropillars and micro-helices that can reversibly bend and swim forward, respectively.

In addition to the printing material and printing strategies, the stimulation regulation can enable the microstructured hydrogels to change their shapes. For instance, Zheng et al. [23] printed some PNIPAm hydrogel microcantilevers incorporated with Fe₃O₄ NPs, allowing the thermally responsive microcantilever matrix to be remotely actuated by NIR light. By giving localized laser, the tips of the microcantilevers move close to each other like a gripper. Similarly, Lee et al. [102] incorporated superparamagnetic iron oxide NPs into PNIPAm-based hydrogel micro-rollers and micro-screws. By regulating the magnetic field, these microstructures move along a designated trajectory.

5.3 Applications

Microstructured hydrogels fabricated by 2PP have a great advantage in microscale applications, including micromachines, micro-sensors, and biomedical areas, as shown in Table 5.

For biological applications, microstructured hydrogels are typically applied to cell or tissue engineering. For example, the pH-responsive hydrogel micro-enclosures based on BSA fabricated by MPL to trap cells like Escherichia coli [137]. The protein-based microchambers serve as habit-culturing cells which can be released when pH is above the isoelectric point of BSA. Similarly, another cell-responsive hydrogel microstructure constructed by MPL from norbornene-modified PVA and peptide crosslinkers can attract cells and subsequently be proteolyzed by protease for the study of cell invasion [136]. Besides, the combination of multi-stimuliresponsive hydrogel pads and inert micropillars can mimic

the behavior of muscles. When one of the stimuli varies, the hydrogel pads swell or deswell, forcing the micropillars to bend reversibly [105].

In addition, 2PP-fabricated micro-hydrogels are commonly used as microrobots or micromachines. The multiply stimuli-responsive hydrogel micromachines, including micro-stents, micro-cages, and micro-umbrellas, can expand or contract when pH, type of solvents, or temperature varies, and have great potential to be applied in biomedical applications like smart intravascular stents and artificial cardiac values [113]. The hydrogel micro-roller (Figure 6(d)) is based on PNIPAm and iron oxide NPs, and this microstructured hydrogel roller can expand or shrink when the temperature varies between 24 and 37°C [102]. By adjusting the frequency of the rotating magnetic field, the 2PP-fabricated microscrew could locomote and steer in the microchannel, which has the potential to be a key enabler for various remote lab-on-a-chip manipulations. A joint-like hydrogel micro-cantilever based on PEGDA can reversely bend when the humidity increases and decreases, simulating joint movement. This sort of 2PP-fabricated hydrogel structure might likely be used to construct humidity-responsive soft robots [89]. Another common application of 2PP-printed microhydrogels is the sensor. The pyramid-like PEGDA microhydrogels are mechanically robust and highly sensitive to pH variation, so they are highly suitable for the application of pH-responsive microdevices, especially micro-biosensors [78]. Besides, the PEGDA micro-hydrogels are humidityresponsive, meaning that they can sense the concentration variations of water vapor in the atmosphere at the microscale [89]. 2PP-printed micro-hydrogels also have other potential applications, like actuators and microfluidic devices. For example, the light-driven hydrogel microcantilevers based on PNIPAm hydrogels and Fe₃O₄ NPs allow the thermal-responsive microcantilever matrix to be remotely actuated by NIR light, showing great potential to biomedical micro-electromechanical systems [23]. Besides, the hydrogel micropillars and micro-helices [26], could be driven by light to bend and swim. It is feasible to use these dynamic micro-structured hydrogels in adaptive micro-devices [138].

6 Challenges for 4D printing of hydrogel structures

Although extensive research studies have contributed to significant advancements in the 4D printing of hydrogels, there is still considerable potential for improvement. The specific challenges in this field differ among the printing techniques, involving the utilization of new hydrogel precursors for 4D printing and the improvement of stimuli-responsiveness and mechanical properties of the 4D-printed hydrogels.

In the field of 4D printing of hydrogel structures using DIW, it is challenging to prepare DIW-printable hydrogel inks since the hydrogel precursors inherently do not have favourable rheological behaviors and desirable printability. Slight pre-crosslinking has been demonstrated to be an effective approach to enhance the printability of some hydrogel inks for 4D printing by DIW [139,140]. For example, part of cellulose chains pre-crosslinked with epichlorohydrin to form the percolating network, can adjust the rheological properties of the cellulose hydrogel ink. Tailoring hydrogel composition by using rheology-modifying additives, [141] and multi-material inks [142] can also improve inks' printability. Moreover, a nanocarrier was proved to be a universal additive for improving the rheological properties of various biomaterials, and this rheology modifier designed for DIW utilized reversible interactions between the polymers and NPs to establish transient physical networks with shear-thinning and selfhealing properties [141]. In addition, the printing resolution of DIW is a disadvantage as compared with SLA and 2PP, limiting some biomedical applications of DIW-printed hydrogel-based structures [143]. The strategy of precisely controlling printing parameters, such as extrusion rate and layer thickness, could contribute to improved resolutions. In addition, incorporating NPs or nanofillers into the hydrogel inks is also capable of printing hydrogels with enhanced mechanical properties [144].

Compared to DIW, SLA and 2PP offer superior printing resolutions, and the printability of photocurable hydrogel precursors is less dependent on their rheological properties. Unlike the 2PP utilizing NIR light laser at 780 nm, SLA typically uses UV or visible light laser, such as wavelength around 365 or 405 nm, which have inferior light penetration capabilities, especially in semi-transparent and opaque photoresists. Insufficient light penetration, especially in the inner regions of large-sized objects, can result in incomplete crosslinking, subsequently diminishing the mechanical properties. To address this, reducing the size of inorganic particles incorporated into the photoresist can improve UV transparency while preventing self-aggregation. For instance, utilizing 10 nm maghemite particles treated with oleic acid in SU-8 photoresists has been shown to enhance transparency in the UV region [145]. Additionally, the SLA and TPP can print the heterogenous structures by regulating the laser dose distribution, but the laser dose difference can cause insufficient polymerization or over-polymerization,

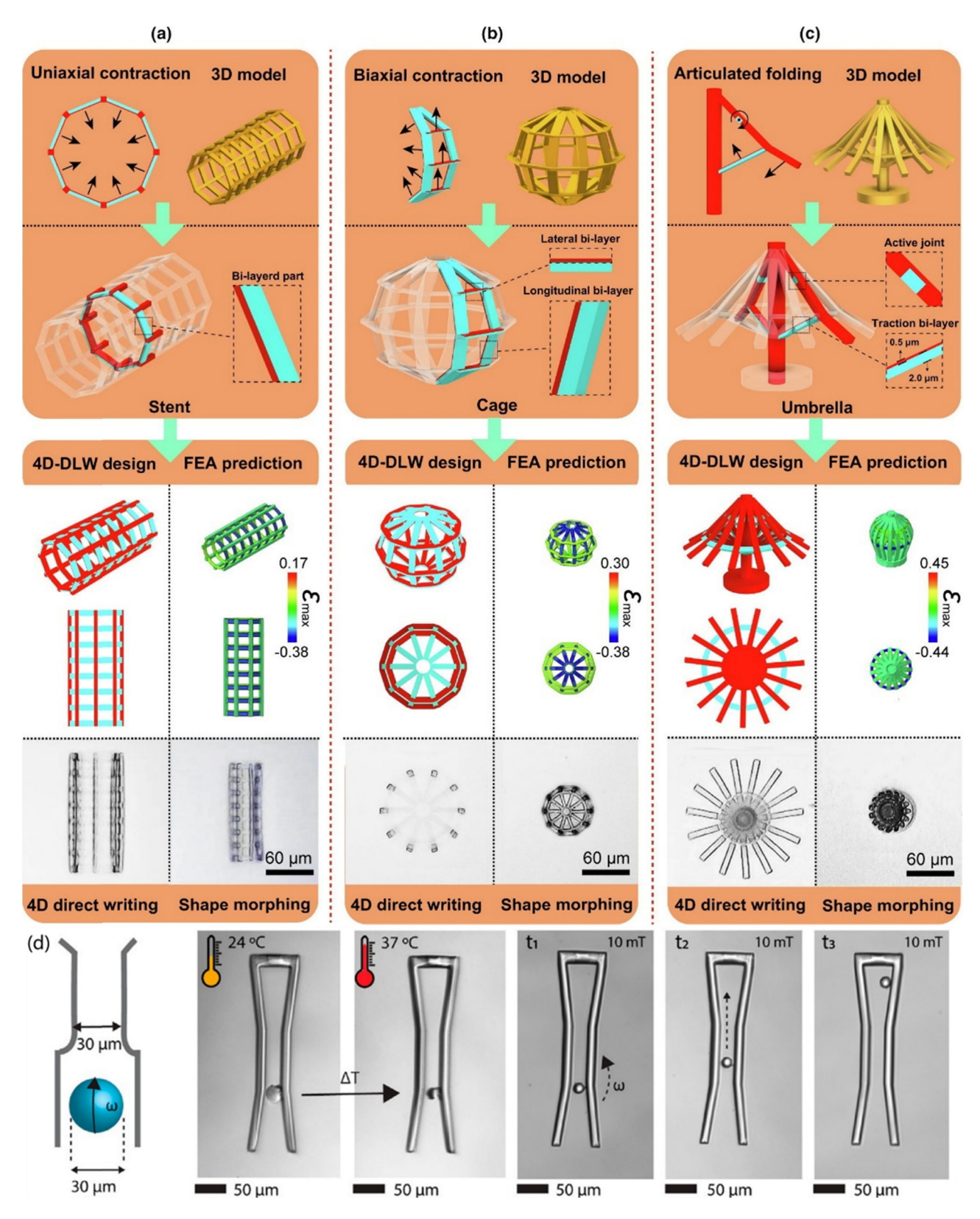


Figure 6: Images for 4D 2PP-printed micro-hydrogels. (a) hydrogel micro-stent, (b) micro-cage which can reversibly contract or expand in uniaxial and biaxial manners, respectively, and (c) reversibly foldable hydrogel micro-umbrella; Reproduced with permission [113]. Copyright, 2019, Elsevier, under the terms of the Creative Commons CC-BY license. (d) Schematic and optical images of the hydrogel micro-roller based on PNIPAm and iron oxide NPs, expansion or shrinkage between 24 and 37°C, and locomotion controlled by a magnetic field. Reproduced with permission [102]. Copyright, 2020. Published by American Chemical Society under the terms of Creative Commons public.

resulting in collapsed or burnt hydrogel structures [146,147]. The utilization of the 4D printing strategy for the fabrication of heterogenous hydrogel structures needs to be further optimized. For example, instead of printing bi-layered hydrogel structures, the strategies of gradient printing by 2PP can be used to tailor the spatial crosslinking gradients in photoresists [148]. This issue could also be addressed by the development of photoresists with wide laser dose ranges of polymerization and the establishment of thresholding models for predicting the threshold of over-polymerization [147]. 2PP-based printing technology, capable of achieving sub-micron printing precision, has enabled the fabrication of intricate and micro-nanostructures but the constrained work area limits the object size [149]. It is also challenging to print large micro-nanostructures via 2PP because defects would be likely to be produced during the long printing time. The uniform and stable photoresists can mitigate this issue, particularly necessitating the PIs to evenly dissolve in the photoresists without aggregation and precipitation. In addition, the hybrid utilization of different printing technologies can combine the advantages of different technologies and may solve this problem [150].

In the application of the 4D-printed hydrogels, DIW has been widely utilized for fabricating hydrogel-based structures for applications such as hydrogel-based flexible devices, [151] and soft robotics [152]. In the field of biomedical applications such as drug delivery, DIW, and SLA are feasible techniques for 4D-printed hydrogel structures. Common materials employed in previous studies include PNIPAm and PEGDA. However, beyond their drug encapsulation and release functionalities, material toxicity remains an important issue, particularly upon degradation. To mitigate this, the development of biomaterials for 4D printing [153] and the use of biocompatible initiators [154] with enhanced initiating efficiency can minimize adverse effects. Despite advances in stimulus-responsive polymers for drug delivery systems, achieving precise control over stimuli such as temperature, pH, and ion responsiveness remains a challenge. Light and magnetic-responsive hydrogels may be alternatives, but they generally rely on inorganic materials, presenting compatibility issues with polymer hydrogel networks and stability challenges in aqueous environments. In this context, the incorporation of polymer-based photothermal materials, for example, conjugated polymers emerges as an appealing choice for fabricating lightresponsive hydrogels [155]. For the flexible device application, DIW stands out as the preferred printing technique because of its capability to print large hydrogel structures and its suitability for various materials. The development of conductive or electric-responsive hydrogels that can

sense and convert environmental stimuli into electrical signals would further promote their applications in hydrogel-based flexible electronics [156,157]. Lastly, in the areas of soft robotics and actuators, extensive research work has been conducted on macro-hydrogels printed by DIW, but the exploration for 4D-printed hydrogels combining rapid responsiveness and mechanical robustness remains limited. The incorporation of nanomaterials may be a solution to enhance mechanical properties while retaining responsiveness. 2PP-printed hydrogels have shown promise for micro-actuators or microrobots with arbitrary and complex architectures, although their practical application is still a work in progress.

7 Conclusion and perspectives

This paper reviews the current additive manufacturing techniques for the 4D printing of hydrogel structures, including SLA, DIW, and 2PP. It summarizes the materials and strategies employed in fabricating dynamic 3D hydrogels, and their applications. More importantly, insights into the selection and utilization of 4D printing strategies tailored to specific functions and applications of the 4Dprinted hydrogel structures were discussed in detail. Using stimuli-responsive materials, multi-material printing, fabricating heterogeneous structures with a single material, and controlling the stimulus are useful strategies for the 4D printing of hydrogels with complex shape changes. DIW has been an essential technique for the 4D printing of hydrogels on the centimeter scale or above, particularly light- or magnetic-responsive hydrogels, and multi-material fabrication. These hydrogels printed by DIW via extra printing strategies show complex shape-changing behavior and are promising for applications such as soft robots. SLA has been the desirable technology for the 4D printing of macrohydrogels from non-extrudable hydrogel precursors, and the 4D-printed hydrogels fabricated by SLA have been demonstrated to be promising for drug delivery. 2PP has been significant in the 4D printing of microscale hydrogels, and these hydrogel-based structures printed by 2PP are likely to be applied as micro-robots.

For the future development of 4D-printed hydrogelbased structures, there are still some challenges and opportunities that are worth further exploration. The fundamental challenge is to trade off a balance between rapid responsiveness and mechanical robustness, and incorporating nanomaterials into hydrogels to enhance the mechanical properties of the resulting composites while preserving their responsiveness holds great promise. In addition, enhancing the printing resolution of DIW remains a key challenge, with potential improvements achievable through optimizing printing parameters and hydrogel ink formulations. Regarding 4D-printed hydrogel structures using SLA and 2PP, many of their applications remain in the research stage with a great deal of effort required for further development.

Acknowledgments: The authors would like to express sincere thanks to the financial support from the Research Committee of The Hong Kong Polytechnic University (Project codes: RHFV and G-UARR). The work described in this paper was partially supported by a grant from the Research Grants Council of the Hong Kong Special Administrative Region, China (Project Nos. PolyU15211221 and PolyU15212523).

Funding information: The authors would like to express sincere thanks to the financial support from the Research Committee of The Hong Kong Polytechnic University (Project codes: RHFV and G-UARR). The work described in this paper was partially supported by a grant from the Research Grants Council of the Hong Kong Special Administrative Region, China (Project Nos. PolyU15211221 and PolyU15212523).

Author contributions: All authors have accepted responsibility for the entire content of this manuscript and approved its submission.

Conflict of interest: The authors state no conflict of interest.

References

DE GRUYTER

- Tibbits, S. 4D printing: multi-material shape change. Architectural [1] Design, Vol. 84, No. 1, 2014, pp. 116-121.
- [2] Ali, M., F. Alam, Y. F. Fah, O. Shiryayev, N. Vahdati, and H. J. Butt. 4D printed thermochromic Fresnel lenses for sensing applications. Composites Part B: Engineering, Vol. 230, 2022, id. 109514.
- [3] Chen, D., Q. Liu, Z. Han, J. Zhang, H. Song, K. Wang, et al. 4D printing strain self-sensing and temperature self-sensing integrated sensor-actuator with bioinspired gradient gaps. Advanced Science, Vol. 7, No. 13, 2020, id. 2000584.
- [4] Wang, Y. and X. Li. 4D printing reversible actuator with strain selfsensing function via structural design. Composites Part B: Engineering, Vol. 211, 2021, id. 108644.
- Garces, I. and C. Ayranci. Active control of 4D prints: Towards 4D [5] printed reliable actuators and sensors. Sensors and Actuators A: Physical, Vol. 301, 2020, id. 111717.
- [6] Hu, X., Z. Ge, X. Wang, N. Jiao, S. Tung, and L. Liu. Multifunctional thermo-magnetically actuated hybrid soft millirobot based on 4D printing. Composites Part B: Engineering, Vol. 228, 2022, id. 109451.
- [7] Zhang, Y.-F., Z. Li, H. Li, H. Li, Y. Xiong, X. Zhu, et al. Fractal-based stretchable circuits via electric-field-driven microscale 3D printing

- for localized heating of shape memory polymers in 4D printing. ACS Applied Materials & Interfaces, Vol. 13, No. 35, 2021, pp. 41414-41423.
- [8] Cheng, T., M. Thielen, S. Poppinga, Y. Tahouni, D. Wood, T. Steinberg, et al. Bio-inspired motion mechanisms: Computational design and material programming of self-adjusting 4D-printed wearable systems. Advanced Science, Vol. 8, No. 13, 2021, id. 2100411.
- [9] Yang, C., J. Luo, M. Polunas, N. Bosnjak, S. T. D. Chueng, M. Chadwick, et al. 4D-printed transformable tube array for highthroughput 3D cell culture and histology. Advanced Materials, Vol. 32, No. 40, 2020, id. 2004285.
- [10] Hwangbo, H., H. Lee, E. J. Roh, W. Kim, H. P. Joshi, S. Y. Kwon, et al. Bone tissue engineering via application of a collagen/hydroxyapatite 4D-printed biomimetic scaffold for spinal fusion. Applied Physics Reviews, Vol. 8, No. 2, 2021, id. 021403.
- [11] Kashyap, D., P. K. Kumar, and S. Kanagaraj. 4D printed porous radiopaque shape memory polyurethane for endovascular embolization. Additive Manufacturing, Vol. 24, 2018, pp. 687-695.
- Wang, Y., H. Cui, Y. Wang, C. Xu, T. J. Esworthy, S. Y. Hann, et al. 4D printed cardiac construct with aligned myofibers and adjustable curvature for myocardial regeneration. ACS Applied Materials & Interfaces, Vol. 13, No. 11, 2021, pp. 12746-12758.
- Zhang, X. N., Q. Zheng, and Z. L. Wu. Recent advances in 3D printing of tough hydrogels: A review. Composites Part B: Engineering, Vol. 238, 2022, id. 109895.
- Khalid, N. N., N. A. Mohd Radzuan, A. B. Sulong, F. Mohd Foudzi, and D. Hui. Adhesion behaviour of 3D printed polyamide-carbon fibre composite filament. Reviews on Advanced Materials Science, Vol. 61, No. 1, 2022, pp. 838-848.
- Li, Y., L. Huang, X. Wang, Y. Wang, X. Lu, Z. Wei, et al. Blending and [15] functionalisation modification of 3D printed polylactic acid for fused deposition modeling. Reviews on Advanced Materials Science, Vol. 62, No. 1, 2023, id. 20230140.
- [16] Patdiya, J. and B. Kandasubramanian. Progress in 4D printing of stimuli responsive materials. Polymer-Plastics Technology and Materials, Vol. 60, No. 17, 2021, pp. 1845-1883.
- [17] Wan, X., Y. He, Y. Liu, and J. Leng. 4D printing of multiple shape memory polymer and nanocomposites with biocompatible, programmable and selectively actuated properties. Additive Manufacturing, Vol. 53, 2022, id. 102689.
- Zhang, C., D. Cai, P. Liao, J.-W. Su, H. Deng, B. Vardhanabhuti, [18] et al. 4D Printing of shape-memory polymeric scaffolds for adaptive biomedical implantation. Acta Biomaterialia, Vol. 122, 2021, pp. 101-110.
- Kim, K., Y. Guo, J. Bae, S. Choi, H. Y. Song, S. Park, et al. 4D printing of hygroscopic liquid crystal elastomer actuators. Small, Vol. 17, No. 23, 2021, id. 2100910.
- [20] Peng, X., S. Wu, X. Sun, L. Yue, S. M. Montgomery, F. Demoly, et al. 4D printing of freestanding liquid crystal elastomers via hybrid additive manufacturing. Advanced Materials, Vol. 34, No. 39, 2022, id. 2204890.
- Li, Y., W. Zheng, B. Li, J. Dong, G. Gao, and Z. Jiang. Double-layer [21] temperature-sensitive hydrogel fabricated by 4D printing with fast shape deformation. J Colloids Surfaces A: Physicochemical Engineering Aspects, Vol. 648, 2022, id. 129307.
- [22] Qu, G., J. Huang, Z. Li, Y. Jiang, Y. Liu, K. Chen, et al. 4D-printed bilayer hydrogel with adjustable bending degree for enteroatmospheric fistula closure. Materials Today Bio, Vol. 16, 2022, id. 100363.
- Zheng, C., F. Jin, Y. Zhao, M. Zheng, J. Liu, X. Dong, et al. Light-[23] driven micron-scale 3D hydrogel actuator produced by two-

- photon polymerization microfabrication. Sensors and Actuators B: Chemical, Vol. 304, 2020, id. 127345.
- [24] Zhao, Q., Y. H. Liang, L. Ren, F. Qiu, Z. H. Zhang, and L. Q. Ren. Study on temperature and near-infrared driving characteristics of hydrogel actuator fabricated via molding and 3D printing. Journal of the Mechanical Behavior of Biomedical Materials, Vol. 78, 2018,
- Yoshida, K., S. Nakajima, R. Kawano, and H. Onoe, Spring-shaped [25] stimuli-responsive hydrogel actuator with large deformation. Sensors and Actuators B: Chemical, Vol. 272, 2018, pp. 361-368.
- [26] Nishiguchi, A., H. Zhang, S. Schweizerhof, M. F. Schulte, A. Mourran, and M. Moller. 4D printing of a light-driven soft actuator with programmed printing density. ACS Applied Materials & Interfaces, Vol. 12, No. 10, 2020, pp. 12176-12185.
- Dong, Q., S. Chen, J. Zhou, J. Liu, Y. Zou, J. Lin, et al. Design of [27] functional vancomycin-embedded bio-derived extracellular matrix hydrogels for repairing infectious bone defects. Nanotechnology Reviews, Vol. 12, No. 1, 2023, id. 20220524.
- Zhang, J., B. Liu, C. Chen, S. Jiang, Y. Zhang, B. Xu, et al. Ultrafast laser-ablated bioinspired hydrogel-based porous gating system for sustained drug release. ACS Applied Materials & Interfaces, Vol. 14, No. 31, 2022, pp. 35366-35375.
- [29] Li, C., Y. Du, H. Lv, J. Zhang, P. Zhuang, W. Yang, et al. Injectable amphipathic artesunate prodrug-hydrogel microsphere as gene/ drug nano-microplex for rheumatoid arthritis therapy. Advanced Functional Materials, Vol. 32, No. 44, 2022, id. 2206261.
- [30] Yang, X., C. Zhang, D. Deng, Y. Gu, H. Wang, and Q. Zhong. Multiple stimuli-responsive mxene - based hydrogel as intelligent drug delivery carriers for deep chronic wound healing. Small, Vol. 18, No. 5, 2022, id. 2104368.
- [31] Phan, V. G., M. Murugesan, H. Huong, T.-T. Le, T.-H. Phan, P. Manivasagan, et al. Cellulose nanocrystals-incorporated thermosensitive hydrogel for controlled release, 3D printing, and breast cancer treatment applications. ACS Applied Materials & Interfaces, Vol. 14, No. 38, 2022, pp. 42812-42826.
- Γ321 Han, C. and W. Guo. Fluorescent noble metal nanoclusters loaded protein hydrogel exhibiting anti-biofouling and self - healing properties for electrochemiluminescence biosensing applications. Small, Vol. 16, No. 45, 2020, id. 2002621.
- **[331** Peng, Z., S. Niu, L. Gui, X. Kuang, F. Li, B. Chen, et al. Wnt3a loaded deformable hydrogel acts as a 3D culture platform for in situ recruitment of stem cells to efficiently repair bone defects via the asymmetric division. Chemical Engineering Journal, Vol. 442, 2022, id. 136163.
- Zhang, Z., S. Gao, Y. Hu, X. Chen, C. Cheng, X. Fu, et al. Ti₃C₂T_x [34] MXene composite 3D hydrogel potentiates mTOR signaling to promote the generation of functional hair cells in cochlea organoids. Advanced Science, Vol. 9, No. 32, 2022, id. 2203557.
- [35] Shen, J., R. Chang, L. Chang, Y. Wang, K. Deng, D. Wang, et al. Light emitting CMC-CHO based self-healing hydrogel with injectability for in vivo wound repairing applications. Carbohydrate Polymers, Vol. 281, 2022, id. 119052.
- Jie, J., D. Mao, J. Cao, P. Feng, and P. Yang. Customized multi-[36] functional peptide hydrogel scaffolds for CAR-T-cell rapid proliferation and solid tumor immunotherapy. ACS Applied Materials & Interfaces, Vol. 14, No. 33, 2022, pp. 37514-37527.
- Yu, F., P. Yang, Z. Yang, X. Zhang, and J. Ma. Double-network hydrogel adsorbents for environmental applications. Chemical Engineering Journal, Vol. 426, 2021, id. 131900.

- Wei, X., H. Chen, D. Lin, H. Xu, J. Wang, J. Zhang, et al. A field study of nano-FeS loaded lignin hydrogel application for Cd reduction, nutrient enhancement, and microbiological shift in a polluted paddy soil. Chemical Engineering Journal, Vol. 451, 2023, id. 138647.
- [39] Zhou, J., F. Zhuo, X. Long, Y. Liu, H. Lu, J. Luo, et al. Bio-inspired, super-stretchable and self-adhesive hybrid hydrogel with SC-PDA/GO-Ca²⁺/PAM framework for high precision wearable sensors. Chemical Engineering Journal, Vol. 447, 2022, id. 137259.
- [40] Ren, X., M. Yang, T. Yang, C. Xu, Y. Ye, X. Wu, et al. Highly conductive PPy-PEDOT: PSS hybrid hydrogel with superior biocompatibility for bioelectronics application. ACS Applied Materials & Interfaces, Vol. 13, No. 21, 2021, pp. 25374-25382.
- [41] Wang, D., F. Yang, L. Cong, W. Feng, C. Wang, F. Chu, et al. Lignincontaining hydrogel matrices with enhanced adhesion and toughness for all-hydrogel supercapacitors. Chemical Engineering Journal, Vol. 450, 2022, id. 138025.
- [42] Jiang, Z., M. L. Tan, M. Taheri, Q. Yan, T. Tsuzuki, M. G. Gardiner, et al. Strong, self-healable, and recyclable visible-light-responsive hydrogel actuators. Angewandte Chemie, Vol. 132, No. 18, 2020, pp. 7115-7122.
- [43] Zavahir, S., P. Sobolčiak, I. Krupa, D. S. Han, J. Tkac, and P. Kasak. Ti₃C₂T_x MXene-based light-responsive hydrogel composite for bendable bilayer photoactuator. Nanomaterials, Vol. 10, No. 7, 2020, id. 1419.
- [44] Han, Z., P. Wang, G. Mao, T. Yin, D. Zhong, B. Yiming, et al. Dual pH-responsive hydrogel actuator for lipophilic drug delivery. ACS Applied Materials & Interfaces, Vol. 12, No. 10, 2020, pp. 12010-12017.
- [45] Ding, H., B. Li, Y. Jiang, G. Liu, S. Pu, Y. Feng, et al. pH-responsive UV crosslinkable chitosan hydrogel via "thiol-ene" click chemistry for active modulating opposite drug release behaviors. Carbohydrate Polymers, Vol. 251, 2021, id. 117101.
- [46] Liu, J., L. Jiang, A. Liu, S. He, and W. Shao. Ultrafast thermoresponsive bilayer hydrogel actuator assisted by hydrogel microspheres. Sensor Actuator B-chemical, Vol. 357, 2022, id. 131434.
- [47] Chen, T., Y. Yang, H. Peng, A. K. Whittaker, Y. Li, Q. Zhao, et al. Cellulose nanocrystals reinforced highly stretchable thermalsensitive hydrogel with ultra-high drug loading. Carbohydrate Polymers, Vol. 266, 2021, id. 118122.
- Ying, Z., Q. Wang, J. Xie, B. Li, X. Lin, and S. Hui. Novel electrically-[48] conductive electro-responsive hydrogels for smart actuators with a carbon-nanotube-enriched three-dimensional conductive network and a physical-phase-type three-dimensional interpenetrating network. Journal of Materials Chemistry C, Vol. 8, No. 12, 2020, pp. 4192-4205.
- [49] Jiang, H., L. Fan, S. Yan, F. Li, H. Li, and J. Tang. Tough and electroresponsive hydrogel actuators with bidirectional bending behavior. Nanoscale, Vol. 11, No. 5, 2019, pp. 2231-2237.
- [50] Manjua, A. C., V. D. Alves, J. O. G. Crespo, and C. A. Portugal. Magnetic responsive PVA hydrogels for remote modulation of protein sorption. ACS Applied Materials & Interfaces, Vol. 11, No. 23, 2019. pp. 21239-21249.
- [51] Chen, H., X. Zhang, L. Shang, and Z. Su. Programmable anisotropic hydrogels with localized photothermal/magnetic responsive properties. Advanced Science, Vol. 9, No. 26, 2022, id. 2202173.
- [52] McCracken, J. M., A. Badea, M. E. Kandel, A. S. Gladman, D. J. Wetzel, G. Popescu, et al. Programming mechanical and physicochemical properties of 3D hydrogel cellular microcultures via

- direct ink writing. Advanced Healthcare Materials, Vol. 5, No. 9, 2016, pp. 1025-1039.
- [53] Chen, J., L. Xu, M. Yang, X. Chen, X. Chen, and W. Hong. Highly stretchable photonic crystal hydrogels for a sensitive mechanochromic sensor and direct ink writing. Chemistry of Materials, Vol. 31, No. 21, 2019, pp. 8918-8926.
- Chan, V., P. Zorlutuna, J. H. Jeong, H. Kong, and R. Bashir. Threedimensional photopatterning of hydrogels using stereolithography for long-term cell encapsulation. Lab on a Chip, Vol. 10, No. 16, 2010, pp. 2062-2070.
- Chan, V., J. H. Jeong, P. Bajaj, M. Collens, T. Saif, H. Kong, et al. Multi-material bio-fabrication of hydrogel cantilevers and actuators with stereolithography. Lab on a Chip, Vol. 12, No. 1, 2012, pp. 88-98.
- Han, D., Z. Lu, S. A. Chester, and H. Lee. Micro 3D printing of a [56] temperature-responsive hydrogel using projection micro-stereolithography. Scientific Reports, Vol. 8, No. 1, 2018, pp. 1-10.
- Solis, D. M. and A. Czekanski. The effect of the printing temperature on 4D DLP printed pNIPAM hydrogels. Soft Matter, Vol. 18, No. 17, 2022, pp. 3422-3429.
- [58] Ding, A., S. J. Lee, S. Ayyagari, R. Tang, C. T. Huynh, and E. Alsberg. 4D biofabrication via instantly generated graded hydrogel scaffolds. Bioactive Materials, Vol. 7, 2022, pp. 324-332.
- [59] Song, J., C. Michas, C. S. Chen, A. E. White, and M. W. Grinstaff. From simple to architecturally complex hydrogel scaffolds for cell and tissue engineering applications: Opportunities presented by two-photon polymerization. Advanced Healthcare Materials, Vol. 9, No. 1, 2020, id. 1901217.
- [60] Lao, Z. X., N. Xia, S. J. Wang, T. T. Xu, X. Y. Wu, and L. Zhang. Tethered and untethered 3d microactuators fabricated by twophoton polymerization: A review. Micromachines, Vol. 12, No. 4,
- Spiegel, C. A., M. Hippler, A. Münchinger, M. Bastmeyer, C. Barner-Kowollik, M. Wegener, et al. 4D printing at the microscale. Advanced Functional Materials, Vol. 30, 2019, id. 26.
- Dong, Y. T., S. C. Wang, Y. J. Ke, L. C. Ding, X. T. Zeng, S. Magdassi, et al. 4D printed hydrogels: Fabrication, materials, and applications. Advanced Materials Technologies, Vol. 5, No. 6, 2020, id. 200034.
- Champeau, M., D. A. Heinze, T. N. Viana, E. R. de Souza, A. C. Chinellato, and S. Titotto. 4D printing of hydrogels: A review. Advanced Functional Materials, Vol. 30, No. 31, 2020, id. 1910606.
- [64] Bakarich, S. E., R. Gorkin, M. I. H. Panhuis, and G. M. Spinks. 4D printing with mechanically robust, thermally actuating hydrogels. Macromolecular Rapid Communications, Vol. 36, No. 12, 2015, pp. 1211-1217.
- [65] Zu, S., Z. Zhang, Q. Liu, Z. Wang, Z. Song, Y. Guo, et al. 4D printing of core-shell hydrogel capsules for smart controlled drug release. Bio-Design Manufacturing, Vol. 5, No. 2, 2022, pp. 294-304.
- Podstawczyk, D., M. Niziol, P. Szymczyk-Ziolkowska, and M. [66] Fiedot-Tobola. Development of thermoinks for 4D direct printing of temperature-induced self-rolling hydrogel actuators. Advanced Functional Materials, Vol. 31, No. 15, 2021, id. 2009664.
- [67] Arslan, H., A. Nojoomi, J. Jeon, and K. Yum. 3D printing of anisotropic hydrogels with bioinspired motion. Advanced Science, Vol. 6, No. 2, 2019, id. 1800703.
- [68] Naficy, S., R. Gately, R. Gorkin III, H. Xin, and G. M. Spinks. 4D printing of reversible shape morphing hydrogel structures.

- Macromolecular Materials and Engineering, Vol. 302, No. 1, 2017, id. 1600212.
- [69] Cheng, Y., K. H. Chan, X.-Q. Wang, T. Ding, T. Li, X. Lu, et al. Directink-write 3D printing of hydrogels into biomimetic soft robots. ACS Nano, Vol. 13, No. 11, 2019, pp. 13176-13184.
- [70] Hippler, M., E. Blasco, J. Qu, M. Tanaka, C. Barner-Kowollik, M. Wegener, et al. Controlling the shape of 3D microstructures by temperature and light. Nature Communications, Vol. 10, No. 1, 2019, id. 232.
- [71] Pelton, R. Poly(N-isopropylacrylamide)(PNIPAM) is never hydrophobic. Journal of ColloidInterface Science, Vol. 348, No. 2, 2010, pp. 673-674.
- [72] de Oliveira, T. E., D. Mukherji, K. Kremer, and P. A. Netz. Effects of stereochemistry and copolymerization on the LCST of PNIPAm. Journal of Chemical Physics, Vol. 146, No. 3, 2017, id. 034904.
- Bischofberger, I. and V. Trappe. New aspects in the phase [73] behaviour of poly-N-isopropyl acrylamide: systematic temperature dependent shrinking of PNIPAm assemblies well beyond the LCST. Scientific Reports, Vol. 5, No. 1, 2015, pp. 1-10.
- Ji, Z. Y., C. Y. Yan, B. Yu, X. Q. Zhang, M. R. Cai, X. Jia, et al. 3D printing of hydrogel architectures with complex and controllable shape deformation. Advanced Materials Technologies, Vol. 4, No. 4, 2019, id. 1800713.
- Shiblee, M. N. I., K. Ahmed, M. Kawakami, and H. Furukawa. 4D printing of shape-memory hydrogels for soft-robotic functions. Advanced Materials Technologies, Vol. 4, No. 8, 2019, id. 1900071.
- [76] Tudor, A., C. Delaney, H. Zhang, A. J. Thompson, V. F. Curto, G.-Z. Yang, et al. Fabrication of soft, stimulus-responsive structures with sub-micron resolution via two-photon polymerization of poly (ionic liquid)s. Materials Today, Vol. 21, No. 8, 2018, pp. 807-816.
- [77] Ofridam, F., M. Tarhini, N. Lebaz, É. Gagnière, D. Mangin, and A. Elaissari. pH-sensitive polymers: Classification and some fine potential applications. Polymers for Advanced Technologies, Vol. 32, No. 4, 2021, pp. 1455-1484.
- [78] Scarpa, E., E. D. Lemma, R. Fiammengo, M. P. Cipolla, F. Pisanello, F. Rizzi, et al. Microfabrication of pH-responsive 3D hydrogel structures via two-photon polymerization of high-molecularweight poly (ethylene glycol) diacrylates. Sensors and Actuators, B: Chemical, Vol. 279, 2019, pp. 418-426.
- [79] Cheng, R., M. Xu, X. Zhang, J. Jiang, Q. Zhang, and Y. Zhao. Hydrogen bonding enables polymer hydrogels with pH-induced reversible dynamic responsive behaviors. Angewandte Chemie International Edition, Vol. 62, No. 23, 2023, id. e202302900.
- [80] Cao, P., L. Tao, J. Gong, T. Wang, Q. Wang, J. Ju, et al. 4D printing of a sodium alginate hydrogel with step-wise shape deformation based on variation of crosslinking density. ACS Applied Polymer Materials, Vol. 3, No. 12, 2021, pp. 6167-6175.
- [81] Lai, J., X. Ye, J. Liu, C. Wang, J. Li, X. Wang, et al. 4D printing of highly printable and shape morphing hydrogels composed of alginate and methylcellulose. Materials Design, Vol. 205, 2021,
- [82] Valentin, T. M., E. M. DuBois, C. E. Machnicki, D. Bhaskar, F. R. Cui, and I. Y. Wong. 3D printed self-adhesive PEGDA-PAA hydrogels as modular components for soft actuators and microfluidics. Polymer Chemistry, Vol. 10, No. 16, 2019, pp. 2015-2028.
- [83] Nguyen, H. T., N. H. Do, H. D. Lac, P. L. Nguyen, and P. K. Le. Synthesis, properties, and applications of chitosan hydrogels as anti-inflammatory drug delivery system. Journal of Porous Materials, Vol. 30, No. 2, 2023, pp. 655-670.

- [84] Zhu, X., C. Yang, Y. Jian, H. Deng, Y. Du, and X. Shi. Ion-responsive chitosan hydrogel actuator inspired by carrotwood seed pod. *Carbohydrate Polymers*, Vol. 276, 2022, id. 118759.
- [85] Khan, S. and N. M. Ranjha. Effect of degree of cross-linking on swelling and on drug release of low viscous chitosan/poly (vinyl alcohol) hydrogels. *Polymer bulletin*, Vol. 71, 2014, pp. 2133–2158.
- [86] Zeng, W., C. Jiang, and D. Wu. Heterogeneity regulation of bilayer polysaccharide hydrogels for integrating pH-and humidityresponsive actuators and sensors. ACS Applied Materials & Interfaces, Vol. 15, No. 12, 2023, pp. 16097–16108.
- [87] Mulakkal, M. C., R. S. Trask, V. P. Ting, and A. M. Seddon. Responsive cellulose-hydrogel composite ink for 4D printing. *Materials & Design*, Vol. 160, 2018, pp. 108–118.
- [88] Jiang, Z., P. D. Shen, M. L. Tan, Q. Yan, J. Viktorova, C. Cementon, et al. 3D and 4D printable dual cross-linked polymers with high strength and humidity-triggered reversible actuation. *Materials Advances*, Vol. 2, No. 15, 2021, pp. 5124–5134.
- [89] Lv, C., X.-C. Sun, H. Xia, Y.-H. Yu, G. Wang, X.-W. Cao, et al. Humidity-responsive actuation of programmable hydrogel microstructures based on 3D printing. Sensors Actuators B: Chemical, Vol. 259, 2018, pp. 736–744.
- [90] Basu, A., A. Saha, C. Goodman, R. T. Shafranek, and A. Nelson. Catalytically initiated gel-in-gel printing of composite hydrogels. ACS Applied Materials & Interfaces, Vol. 9, No. 46, 2017, pp. 40898–40904.
- [91] Han, D., Y. P. Wang, C. Yang, and H. Lee. Multimaterial printing for cephalopod-inspired light-responsive artificial chromatophores. ACS Applied Materials & Interfaces, Vol. 13, No. 11, 2021, pp. 12735–12745.
- [92] Horák, J., A. Nikiforov, F. Krčma, M. Březina, Z. Kozáková, L. Dostál, et al. Synthesis of Ag and Cu nanoparticles by plasma discharge in inorganic salt solutions. *Nanotechnology Reviews*, Vol. 12, No. 1, 2023, id. 20220549.
- [93] Ruban, P., L. Joji, Reddy S. J, R. Manickam, R. Rathinam, S. Rajkumar, S. Sharma, et al. Green synthesis, characterizations, and antibacterial activity of silver nanoparticles from Themeda quadrivalvis, in conjugation with macrolide antibiotics against respiratory pathogens. *Reviews on Advanced Materials Science*, Vol. 62, No. 1, 2023, id. 20220301.
- [94] Sharma, S., P. Sudhakara, and E. M. T. Eldin. Green synthesis, characterizations, and antibacterial activity of silver nanoparticles. *Reviews on Advanced Materials Science*, Vol. 62, 2023, id. 20220301.
- [95] Maamoun, W., M. I. Badawi, A. A. Aly, and Y. Khedr. Nanoparticles in enhancing microwave imaging and microwave Hyperthermia effect for liver cancer treatment. *Reviews on Advanced Materials Science*, Vol. 60, No. 1, 2021, pp. 223–236.
- [96] Yan, J., G. Pan, W. Lin, Z. Tang, J. Zhang, J. Li, et al. Multiresponsive graphene quantum dots hybrid self-healing structural color hydrogel for information encoding and encryption. *Chemical Engineering Journal*, Vol. 451, 2023, id. 138922.
- [97] Shi, Y., Z. Wang, X. Zhou, C. Lin, C. Chen, B. Gao, et al. Preparation of a 3D printable high-performance GelMA hydrogel loading with magnetic cobalt ferrite nanoparticles. Frontiers in Bioengineering Biotechnology, Vol. 11, 2023, id. 1132192.
- [98] Zemtsova, E., A. Ponomareva, A. Arbenin, and V. Smirnov. Structural organization of themagnetic part of smart material based on nanoparticles of iron or magnetite in pores of mcm-41 mesoporous silica for target drug delivery. *Reviews on Advanced Materials Science*, Vol. 57, No. 2, 2018, pp. 175–182.

- [99] Simińska-Stanny, J., M. Nizioł, P. Szymczyk-Ziółkowska, M. Brożyna, A. Junka, A. Shavandi, et al. 4D printing of patterned multimaterial magnetic hydrogel actuators. *Additive Manufacturing*, Vol. 49, 2022, id. 102506.
- [100] Podstawczyk, D., M. Niziol, P. Szymczyk, P. Wisniewski, and A. Guiseppi-Elie. 3D printed stimuli-responsive magnetic nanoparticle embedded alginate-methylcellulose hydrogel actuators. Additive Manufacturing, Vol. 34, 2020, id. 101275.
- [101] Ansari, M. A., R. Govindasamy, M. Y. Begum, M. Ghazwani, A. Alqahtani, M. N. Alomary, et al. Bioinspired ferromagnetic CoFe₂O₄ nanoparticles: Potential pharmaceutical and medical applications. *Nanotechnology Reviews*, Vol. 12, No. 1, 2023, id. 20230575.
- [102] Lee, Y. W., H. Ceylan, I. C. Yasa, U. Kilic, and M. Sitti. 3D-printed multi-stimuli-responsive mobile micromachines. ACS Applied Materials & Interfaces, Vol. 13, No. 11, 2021, pp. 12759–12766.
- [103] Nikolovski, D., M. Jeremic, J. Paunovic, D. Vucevic, T. Radosavljevic, S. Radojević-Škodrić, et al. Application of iron oxide nanoparticles in contemporary experimental physiology and cell biology research. *Reviews on Advanced Materials Science*, Vol. 53, No. 1, 2018, pp. 74–78.
- [104] Narupai, B., P. T. Smith, and A. Nelson. 4D printing of multistimuli responsive protein – based hydrogels for autonomous shape transformations. *Advanced Functional Materials*, Vol. 31, No. 23, 2021, id. 2011012.
- [105] Zarzar, L. D., P. Kim, M. Kolle, C. J. Brinker, J. Aizenberg, and B. Kaehr. Direct writing and actuation of three-dimensionally patterned hydrogel pads on micropillar supports. *Angewandte Chemie*, Vol. 123, No. 40, 2011, pp. 9528–9532.
- [106] Dutta, S. and D. Cohn. Temperature and pH responsive 3D printed scaffolds. *Journal of Materials Chemistry B*, Vol. 5, No. 48, 2017, pp. 9514–9521.
- [107] Lei, Z., Q. Wang, and P. Wu. A multifunctional skin-like sensor based on a 3D printed thermo-responsive hydrogel. *Materials Horizons*, Vol. 4, No. 4, 2017, pp. 694–700.
- [108] Wang, L. Q., F. R. Liu, J. Qian, Z. L. Wu, and R. Xiao. Multiresponsive PNIPAM-PEGDA hydrogel composite. Soft Matter, Vol. 17, No. 46, 2021, pp. 10421–10427.
- [109] Go, G., Z. Jin, J.-O. Park, and S. Park. A thermo-electromagnetically actuated microrobot for the targeted transport of therapeutic agents. *International Journal of Control, Automation Systems*, Vol. 16, No. 3, 2018, pp. 1341–1354.
- [110] Li, H., G. Go, S. Y. Ko, J.-O. Park, and S. Park. Magnetic actuated pH-responsive hydrogel-based soft micro-robot for targeted drug delivery. *Smart Materials and Structures*, Vol. 25, No. 2, 2016, id. 027001.
- [111] Zhao, H., Y. Huang, F. Lv, Liu, L., Q. Gu, and S. Wang. Biomimetic 4D-printed breathing hydrogel actuators by nanothylakoid and thermoresponsive polymer networks. *Advanced Functional Materials*, Vol. 31, No. 49, 2021, id. 2105544.
- [112] Odent, J., S. Vanderstappen, A. Toncheva, E. Pichon, T. J. Wallin, K. Y. Wang, et al. Hierarchical chemomechanical encoding of multi-responsive hydrogel actuators via 3D printing. *Journal of Materials Chemistry A*, Vol. 7, No. 25, 2019, pp. 15395–15403.
- [113] Jin, D., Q. Chen, T. Y. Huang, J. Huang, L. Zhang, and H. Duan. Four-dimensional direct laser writing of reconfigurable compound micromachines. *Materials Today*, Vol. 32, 2020, pp. 19–25.
- [114] Skylar-Scott, M. A., J. Mueller, C. W. Visser, and J. A. Lewis. Voxelated soft matter *via* multimaterial multinozzle 3D printing. *Nature*, Vol. 575, No. 7782, 2019, pp. 330–335.

- Choi, Y., C. Kim, H. S. Kim, C. Moon, and K. Y. Lee. 3D Printing of dynamic tissue scaffold by combining self-healing hydrogel and self-healing ferrogel. Colloids and Surfaces B: Biointerfaces, Vol. 208, 2021, id. 112108.
- [116] Schwab, A., R. Levato, M. D'Este, S. Piluso, D. Eglin, and J. Malda. Printability and shape fidelity of bioinks in 3D bioprinting. Chemical Reviews, Vol. 120, No. 19, 2020, pp. 11028-11055.
- Smith, P. T., A. Basu, A. Saha, and A. Nelson, Chemical modification and printability of shear-thinning hydrogel inks for directwrite 3D printing. Polymer, Vol. 152, 2018, pp. 42-50.
- Wang, J. L., Y. Liu, S. H. Su, J. H. Wei, S. E. Rahman, F. Ning, et al. Ultrasensitive wearable strain sensors of 3D printing tough and conductive hydrogels. Polymers, Vol. 11, No. 11, 2019, id. 1873.
- [119] Podstawczyk, D., M. Nizioł, P. Szymczyk-Ziółkowska, and M. Fiedot-Toboła. Development of thermoinks for 4D direct printing of temperature - induced self-rolling hydrogel actuators. Advanced Functional Materials, Vol. 31, No. 15, 2021, id. 2009664.
- [120] Liaw, C. Y., J. Pereyra, A. Abaci, S. Ji, and M. Guvendiren. 4D printing of surface morphing hydrogels. Advanced Materials Technologies, Vol. 7, No. 6, 2022, id. 2101118.
- Wu, D., J. Song, Z. Zhai, M. Hua, C. Kim, I. Frenkel, et al. Visualizing morphogenesis through instability formation in 4-D printing. ACS Applied Materials & Interfaces, Vol. 11, No. 50, 2019, pp. 47468-47475.
- [122] Guo, J. H., R. R. Zhang, L. N. Zhang, and X. D. Cao. 4D printing of robust hydrogels consisted of agarose nanofibers and polyacrylamide. ACS Macro Letters, Vol. 7, No. 4, 2018, pp. 442-446.
- [123] Uchida, T. and H. Onoe. 4D printing of multi-hydrogels using direct ink writing in a supporting viscous liquid. Micromachines, Vol. 10, No. 7, 2019, id. 433.
- [124] Gladman, A. S., E. A. Matsumoto, R. G. Nuzzo, L. Mahadevan, and J. A. Lewis. Biomimetic 4D printing. Nature Materials, Vol. 15, No. 4, 2016, id. 413.
- [125] Yang, Y., L. Guan, H. Jiang, L. Duan, and G. Gao. A rapidly responsive photochromic hydrogel with high mechanical strength for ink-free printing. Journal of Materials Chemistry C, Vol. 6, No. 28, 2018, pp. 7619-7625.
- Karis, D. G., R. J. Ono, M. Zhang, A. Vora, D. Storti, M. A. Ganter, et al. Cross-linkable multi-stimuli responsive hydrogel inks for direct-write 3D printing. Polymer Chemistry, Vol. 8, No. 29, 2017, pp. 4199-4206.
- [127] Schmidleithner, C. and D. M. Kalaskar. Stereolithography, IntechOpen, London, UK, 2018.
- [128] Pelluau, T., T. Brossier, M. Habib, S. Sene, G. Félix, J. Larionova, et al. 4D printing nanocomposite hydrogel based on PNIPAM and Prussian blue nanoparticles using stereolithography. Macromolecular Materials Engineering, Vol. 309, No. 3, 2023, id. 2300305.
- [129] Tomal, W. and J. Ortyl. Water-soluble photoinitiators in biomedical applications. Polymers, Vol. 12, No. 5, 2020, id. 1073.
- Nguyen, A. K. and R. J. Narayan. Two-photon polymerization for biological applications. Materials Today, Vol. 20, No. 6, 2017, pp. 314-322.
- [131] Huang, Z., G. C. P. Tsui, Y. Deng, and C. Y. Tang. Two-photon polymerization nanolithography technology for fabrication of stimulus-responsive micro/nano-structures for biomedical applications. Nanotechnology Reviews, Vol. 9, No. 1, 2020, pp. 1118-1136.
- [132] Kolb, C., N. Lindemann, H. Wolter, and G. Sextl. 3D-printing of highly translucent ORMOCER® - based resin using light absorber

- for high dimensional accuracy. Journal of Applied Polymer Science, Vol. 138, No. 3, 2021, id. 49691.
- [133] Hua, M., D. Wu, S. Wu, Y. Ma, Y. Alsaid, and X. He. 4D printable tough and thermoresponsive hydrogels. ACS Applied Polymer Materials, Vol. 13, No. 11, 2020, pp. 12689-12697.
- [134] He, Y. Y., R. Yu, X. P. Li, M. W. Zhang, Y. Zhang, X. Yang, et al. Digital light processing 4D printing of transparent, strong, highly conductive hydrogels. ACS Applied Materials & Interfaces, Vol. 13, No. 30, 2021, pp. 36286-36294.
- [135] Marschner, D. E., S. Pagliano, P. H. Huang, and F. Niklaus. A methodology for two-photon polymerization micro 3D printing of objects with long overhanging structures. Additive Manufacturing, Vol. 66, 2023, id. 103474.
- Г1361 Oin, X. H., X. Wang, M. Rottmar, B. I. Nelson, and K. Maniura-Weber, Near-infrared light-sensitive polyvinyl alcohol hydrogel photoresist for spatiotemporal control of cell-instructive 3D microenvironments. Advanced Materials, Vol. 30, No. 10, 2018, id. 1705564.
- Kaehr, B. and J. B. Shear. Multiphoton fabrication of chemically responsive protein hydrogels for microactuation. Proceedings of the National Academy of Sciences, Vol. 105, No. 26, 2008, pp. 8850-8854.
- [138] Wang, J. Y., F. Jin, X. Z. Dong, J. Liu, and M. L. Zheng. Flytrap inspired pH-Driven 3D hydrogel actuator by femtosecond laser microfabrication. Advanced Materials Technologies, Vol. 7, No. 8, 2022, id. 2200276.
- Falcone, G., P. Mazzei, A. Piccolo, T. Esposito, T. Mencherini, R. P. [139] Aquino, et al. Advanced printable hydrogels from pre-crosslinked alginate as a new tool in semi solid extrusion 3D printing process. Carbohydrate Polymers, Vol. 276, 2022, id. 118746.
- Guo, J., Q. Li, R. Zhang, B. Li, J. Zhang, L. Yao, et al. Loose precross-linking mediating cellulose self-assembly for 3D printing strong and tough biomimetic scaffolds. Biomacromolecules, Vol. 23, No. 3, 2022, pp. 877-888.
- [141] Guzzi, E. A., G. Bovone, and M. W. Tibbitt. Universal nanocarrier ink platform for biomaterials additive manufacturing. Small, Vol. 15, No. 51, 2019, id. 1905421.
- [142] Xu, B., H. Wang, Z. Luo, J. Yang, and Z. Wang. Multi-material 3D printing of mechanochromic double network hydrogels for ondemand patterning. ACS Applied Materials & Interfaces, Vol. 15, No. 8, 2023, pp. 11122-11130.
- [143] Yuk, H. and X. Zhao. A new 3D printing strategy by harnessing deformation, instability, and fracture of viscoelastic inks. Advanced Materials, Vol. 30, No. 6, 2018, id. 1704028.
- [144] Mondal, D. and T. L. Willett. Mechanical properties of nanocomposite biomaterials improved by extrusion during direct ink writing. Journal of the Mechanical Behavior of Biomedical Materials, Vol. 104, 2020, id. 103653.
- [145] Gach, P. C., C. E. Sims, and N. L. Allbritton. Transparent magnetic photoresists for bioanalytical applications. Biomaterials, Vol. 31, No. 33, 2010, pp. 8810-8817.
- Matheuse, F., K. Vanmol, J. Van Erps, W. De Malsche, H. Ottevaere, [146] and G. Desmet. On the potential use of two-photon polymerization to 3D print chromatographic packed bed supports. Journal of Chromatography A, Vol. 1663, 2022, id. 462763.
- Kim, H. and S. K. Saha. Defect control during femtosecond projection two-photon lithography. Procedia Manufacturing, Vol. 48, 2020, pp. 650-655.
- [148] Mao, A., P. Fan, L. Constantin, N. Li, X. Huang, B. Cui, et al. Forming three-dimensional micro-objects using two-dimensional

26

- gradient printing. *Applied Materials Today*, Vol. 28, 2022, id. 101538.
- [149] Zheng, L., K. Kurselis, A. El-Tamer, U. Hinze, C. Reinhardt, L. Overmeyer, et al. Nanofabrication of high-resolution periodic structures with a gap size below 100 nm by two-photon polymerization. *Nanoscale Research Letters*, Vol. 14, 2019, pp. 1–9.
- [150] Jin, J., F. Zhang, Y. Yang, C. Zhang, H. Wu, Y. Xu, et al. Hybrid multimaterial 3D printing using photocuring-while-dispensing. *Small*, 2023, id. 2302405.
- [151] Hao, F., X. Maimaitiyiming, and S. Sun. 3D printed multifunctional self-adhesive and conductive polyacrylamide/chitosan/sodium carboxymethyl cellulose/CNT hydrogels as flexible sensors. *Macromolecular Chemistry Physics*, Vol. 224, No. 2, 2023, id. 2200272.
- [152] Zhou, G.-X., Y.-G. Yu, Z. H. Yang, D. C. Jia, P. Poulin, Y. Zhou, et al. 3D printing graphene oxide soft robotics. ACS Nano, Vol. 16, No. 3, 2022, pp. 3664–3673.
- [153] Lin, C., Z. Huang, Q. Wang, Z. Zou, W. Wang, L. Liu, et al. Massproducible near-body temperature-triggered 4D printed shape

- memory biocomposites and their application in biomimetic intestinal stents. *Composites Part B: Engineering*, Vol. 256, 2023, id. 110623.
- [154] Fan, Y., W. Wu, N. Xie, Y. Huang, H. Wu, J. Zhang, et al.
 Biocompatible engineered erythrocytes as plasmonic sensor initiators for high-sensitive screening of non-small cell lung cancer-derived exosomal miRNA in an integrated system.
 Biosensors Bioelectronics, Vol. 219, 2023, id. 114802.
- [155] Huang, Z., G. C. P. Tsui, Y. Deng, C. Y. Tang, M. Yang, M. Zhang, et al. Bioinspired near-infrared light-induced ultrafast soft actuators with tunable deformation and motion based on conjugated polymers/liquid crystal elastomers. *Journal of Materials Chemistry C*, Vol. 10, No. 35, 2022, pp. 12731–12740.
- [156] Tognato, R., A. R. Armiento, V. Bonfrate, R. Levato, J. Malda, M. Alini, et al. A stimuli-responsive nanocomposite for 3D anisotropic cell-guidance and magnetic soft robotics. *Advanced Functional Materials*, Vol. 29, No. 9, 2019, id. 1804647.
- [157] Ding, Z., C. Yuan, X. Peng, T. Wang, H. J. Qi, and M. L. Dunn. Direct 4D printing *via* active composite materials. *Science Advances*, Vol. 3, No. 4, 2017, id. e1602890.